VAMAS

Technical Working Area 13
Low Cycle Fatigue

RECENT INTERCOMPARISONS ON LOW CYCLE FATIGUE AND ALIGNMENT MEASUREMENTS

Report No. 41
ISSN 1016-2186
February 2003

The Versailles Project on Advanced Materials and Standards supports trade in high technology products through international collaborative projects aimed at providing the technical basis for drafting codes of practice and specifications for advanced materials. The scope of the collaboration embraces all agreed aspects of enabling science and technology - databases, test methods, design standards, and materials technology - which are required as a precursor to the drafting of standards for advanced materials. VAMAS activity emphasizes collaboration on pre-standards measurement research, intercomparison of test results, and consolidation of existing views on priorities for standardization action. Through this activity, VAMAS fosters the development of internationally acceptable standards for advanced materials by the various existing standards development organizations.

• Canada • France • Germany • Italy • Japan • UK • USA • EC •

VAMAS

Technical Working Area 13
Low Cycle Fatigue

RECENT INTERCOMPARISONS ON LOW CYCLE FATIGUE AND ALIGNMENT MEASUREMENTS

Dr. Fathy Kandil
EuroTest Solutions Ltd
PO Box 1226, Kingston, Surrey KT2 5YJ, UK
E-mail: fathy.Kandil@eurotest-solutions.co.uk

Report No. 41
ISSN 1016-2186
February 2001

CONTENTS

Recent Intercomparisons on Low Cycle Fatigue and Alignment Measurements

Dr. Fathy Kandil
EuroTest Solutions, UK

ABSTRACT

This report gives a summary of some of the findings from the EC/VAMAS collaborative study: *'Quantifying Data Uncertainties and the Validation of a Code of Practice for the Measurements of Bending in Uniaxial Fatigue Test Pieces'*, which was partly funded by the Commission of European Communities through the Standards, Measurement and Testing Programme, Project MAT1-CT94-0079.

It provides an overview of the work undertaken and describes the main achievements including the development and validation of a new measurement procedure for the verification of alignment of uniaxial test machines.

Procedures were developed for quantifying uncertainties in strain-controlled or stress-controlled low cycle fatigue (LCF) lifetime data. The developed procedures were applied to experimental data from inter-comparison exercises.

Novel tests that were performed for the first time included LCF tests at elevated temperature with deliberately introduced levels of specimen bending and the measurement of specimen bending under plastic conditions.

Recommendations made as a result of this work include the use of Class 5 alignment, measured in accordance with the new procedure, as the standard required for quality fatigue testing.

PROJECT PARTICIPANTS

The following organisations have contributed to Project MAT1-CT94-0079[1].

Partners

Dr F A Kandil, National Physical Laboratory (NPL), UK, **Project Co-ordinator**

Dr Ing A Scholz, University of Darmstadt (IFW), Germany

Mr J Lindblom, Institutet för Metallforskning (SIMR), Sweden

Mr K Schreiber, BMW Rolls-Royce (BRR), Germany

Ing M A Lont, TNO Institute of Industrial Technology (TNO), The Netherlands

Dr M Marchionni, Consiglio Nazionale delle Riceche (CNR-TEMPE), Italy

Dr G Marquis, VTT Manufacturing Technology (VTT), Finland

Dr K Yamaguchi, National Research Institute for Metals (NRIM), Japan

Associate Partners

Mr N Clarke, Rolls-Royce plc, UK

Dr J Devlukia, Rover Group Ltd, UK

Dr R D Lohr, Instron Ltd, UK

Dr A S Nadkarni, Materials Engineering & Testing Ltd, UK

Dr J Monaghan, Materials Ireland, Ireland

Dr V Bicego, CISE SPA, Italy

Mr P Bontempi, ENEL SPA, Italy

Dr A M[a] Irisarri, INASMET R&D, Spain

Dr.-Ing P Heuler, Industrieanlagen-Betriebsgellschaft GmbH, Germany

Dr S R Holdsworth, GEC Alsthom Turbine Generators Ltd, UK

Mr G Thauvin, GEC Alsthom Ltd, France

Dr T Hollstein, Fraunhofer-Institut für Werkstoffmechanik, Germany

Dr.-Ing K F Stärk, ABB Kraftwerke AG, Switzerland

Prof Dr Arzt, Max-Plank-Institut für Metallforschung, Germany

Dr -Ing K Maile, MPA Stuttgart, Germany

Dipl.-Ing. Y Pan/Dr T -U Kern, Siemens AG KWU, Germany

Mr M W Spindler, Nuclear Electric plc, UK

Dr.-Ing B Melzer, Siempelkamp Ptüf- und Gutachter-Gesellschaft mbH, Germany

Mr M Gomez/ Mr A Correia da Cruz, Instituto de Soldadura e Qualidade, Portugal

Mr A V Holt, Mitsui Babcock Energy Ltd, UK

SYMBOLS AND ABBREVIATIONS

b	local bending strain (= local strain - average strain)
CoP	*Code of Practice for the Measurement of Bending in Uniaxial Low Cycle Fatigue Testing*, Reference 7.
c	distance on the specimen surface between the location of the major crack initiation site and the specimen's lower shoulder edge (see Fig. 1b for an illustration)
c_o	distance on the specimen surface between the location of the major crack initiation site and the centre of the specimen (= $c - 0.5L_{profile}$, see Fig. 1b)
d	specimen diameter
$E_{1/4}$	the modulus of elasticity determined on the initial loading of the first cycle
E_o	the modulus of elasticity determined prior to the start of the test
E_1, E_2	the values of the modulus of elasticity determined on the unloading and loading segments, respectively, of the stress-strain hysteresis loop nearest to mid-life (see Fig. 1a for an illustration)
F	axial force
G_1, G_2, etc.	strain gauge numbers; see Fig. 2 for the recommended numbering system.
L	specimen's overall length
$L_{profile}$	profiled length (see Fig. 1b)
LCF	Low Cycle Fatigue
l_e	extensometer's gauge length
l_g	strain-gauge axial separation (= 0.75 l_p, see Fig. 2 for an illustration)
l_p	parallel length
N_{25}	number of cycles to failure corresponding to 25% drop in maximum stress

N_f	number of cycles to failure
N_{fmax}	the maximum number of cycles to failure in a data set under the same nominal conditions
N_{fmin}	the minimum number of cycles to failure in a data set under the same nominal conditions
O_1 to O_4	specimen orientations (about its longitudinal axis) defined by the location of G_1 with respect to the R-direction; see Fig. 3
R	fillet radius at the ends of the parallel length
R-direction	fixed reference direction with respect to the testing machine. Typically it is the direction from the centre of the grips towards the front of the machine (see Fig. 3)
S_1, S_2, etc.	locations in space that correspond to strain gauges G_1, G_2, etc. in orientation O_1
WP	Work Package
α	slope of the tangent to the log $\Delta\varepsilon_t$ vs log N_f curve
β	maximum percent bending on a given bending measurement plane
β_{1000}	maximum percent bending corresponding to an axial strain, ε_o, of 1000 microstrain
β_{av}	the average of the β_{max} values obtained at all 4 orientations or any 2 diametrically-opposite orientations (e.g. O_1 and O_2)
β_{max}	the maximum percent bending measured on the specimen's surface
ε_o	axial strain
ε_{bk}	maximum bending strain at the maximum peak strain in the fatigue cycle
ε_{bv}	maximum bending strain at the minimum peak strain in the fatigue cycle
ε_{bmax}	the maximum bending strain measured on the specimen's surface
$\Delta\varepsilon_b$	bending strain range (= ε_{bk} - ε_{bv})
$\Delta\varepsilon_t$	total strain range
$\Delta\varepsilon_p$	plastic strain range (= width of hysteresis loop at mean stress; see Fig. 1)
$\Delta\varepsilon_e$	elastic strain range (=$\Delta\varepsilon_t$ - $\Delta\varepsilon_p$)
θ	angle of the maximum bending strain vector with respect to the R-direction (measured in clockwise direction when seen from above)
θ_c	angle (clockwise seen from above) on the specimen's cross section of the location of the major crack initiation site with respect to the R-Direction (see Fig. 1 b)
σ_m	mean stress
σ_{max}	maximum stress
σ_{min}	minimum stress
$\Delta\sigma$	stress range
ψ	Bending Reversibility Parameter [= abs ($\Delta\varepsilon_b$ / $\Delta\varepsilon_o$)]

1. INTRODUCTION

This report gives a summary of some of the findings from the EC/VAMAS collaborative study [1], which was partly funded by the Commission of European Communities through the Standards, Measurement and Testing Programme, Project MAT1-CT94-0079. An earlier EC/VAMAS inter-comparison on low cycle fatigue at elevated temperature [2] showed that the variability in fatigue life data produced by different laboratories can be alarmingly high (with a factor of N_{fmax}/N_{fmin} ranging from 2 to 60, depending on the material and the test conditions) compared with the repeatability within individual laboratories that was typically within a factor of 2. This had highlighted serious concerns regarding the reliability of design data generated from a single laboratory, and how to quantify the uncertainties in such measurements.

The main objective of the present study was to address these issues and quantify the main sources of uncertainty in LCF testing previously identified [3-6], including specimen bending and errors in the strain and temperature measurements. The approach adopted was based on developing uncertainty evaluation protocols and then comparing the experimental results with the theoretical estimates. This has enabled the provision of recommendations for a harmonised approach towards best testing practices for LCF testing. Included in the methodology is a definition of the mandatory statement of uncertainty required by accreditation authorities and customers.

Another major aim of the present work was to validate the recommendations of the NPL "*Code of Practice for the Measurement of Bending in Uniaxial Low Cycle Fatigue Testing*", hereafter referred to as the CoP [7]. The CoP has so far been adopted by 3 international draft standards [8-10].

2. MEASUREMENTS OF SPECIMEN BENDING

The CoP recommends the use of strain-gauged specimens equipped with 8 gauges (2 sets of 4). This is based on the premise that, regardless of the cause of bending, the maximum bending strain will always occur near the ends of the specimen's parallel length. The strains measured by the middle set of gauges can therefore be deduced from the other 2 and significant savings of cost and effort can, therefore, be made if only 2 sets of gauges are used.

The primary aims in this part of the validation exercise were to:

1 verify the hypothesis that 8 gauges are always sufficient for the measurement,
2 validate the CoP procedure for elastic bending measurement,
3 validate the CoP procedure for plastic bending measurement,
4 establish the minimum requirements for a meaningful and cost effective alignment measurement,
5 assess current European capabilities for achieving good alignment, and
6 specify recommended limits for machine alignment for fatigue testing.

To this end, it was decided to carry out 2 inter-comparison exercises involving 2 different laboratory groups as follows:

Inter-Laboratory Exercise 1	Inter-Laboratory Exercise 2
• 7 laboratories • 2 materials • 12 strain gauges • 4 measurement orientations	• 6 laboratories • 2 materials • 8 strain gauges • 2 measurement orientations

2.1 Materials

The materials chosen for this exercise were Nimonic 101 and an aluminium alloy Al 6063. They were selected to allow a comparison of the results from specimens made of a harder material (the Nimonic 101) with those from a softer material (the aluminium alloy). The behaviour of a softer material would resemble that of a harder one at elevated temperature. All measurements were made at ambient temperature and in accordance with the appropriate procedure in the CoP (Procedure A for elastic bending or Procedure B for plastic bending).

Only one batch of the Nimonic 101 (IN597) alloy, cast identification number HLN877, [2] was used in the present tests. This material was comprehensively characterised and checked for homogeneity in respect of composition, microstructure and tensile properties. Table 1 provides a summary of the composition, physical and mechanical properties of the material (as supplied by the manufacturer). The bar stock was solution-treated, aged and in the form of round bars with a nominal diameter of 25 mm. The bars were then cut into blanks, mostly 125 mm long, but some had to be cut to different lengths to suit specific test system requirements.

2.2 Inter-Laboratory Exercise 1

2.2.1 Participating laboratories

The organisations that participated in this exercise were:

BMW Rolls-Royce AeroEngines, Germany
Consiglio Nazionale delle Ricerche - TEMPE, Italy
Institut für Werkstoffkunde -TU Darmstadt, Germany
National Physical Laboratory, United Kingdom
Swedish Institute for Metals, Sweden
TNO Institute of Industrial Technology, The Netherlands
VTT Manufacturing Technology, Finland.

The codes assigned to each partner were chosen at random to preserve anonymity. Tables 2 and 3 include the details of the test equipment, alignment cell dimensions and the strain gauges used by each participant.

2.2.2 Measurement procedures

Each participant machined and strain-gauged its own specimens according to the instructions shown in the CoP. As can be seen in Table 2, all the specimens were cylindrical in geometry and had the same dimensions for the reduced section (7.5 mm diameter, 16.2 mm parallel length and 25 mm transition radius) except those for Lab D, which had a slightly larger diameter and a slightly longer parallel length.

The measurements were performed on specimens manufactured of Nimonic 101 and aluminium alloy 6063 (2 from each material). The Nimonic 101 specimens were ground and the aluminium alloy were turned. Each specimen was prepared with 12 gauges (3 sets of 4), which were selected and bonded to the alignment cells according to the recommendations in the CoP. The measurements were performed at 4 specimen orientations as shown in Fig. 3.

Each participating laboratory carried out a total of 4 measurements as follows:

Elastic measurements (Procedure A)

1. Nimonic 101, 4 orientations, ε_o values in the range 0 and 1500 microstrain, in tension and in compression.

2. Al 6063, 4 orientations, ε_o values in the range 0 and 1000 microstrain, in tension and in compression.

Plastic measurements (Procedure B)

3. Nimonic 101, 1 orientation, ε_o values in the range 2000 and 10,000 microstrain, in tension and in compression.

4. Al 6063, 1 orientation, ε_o values in the range 1500 and 10,000 microstrain, in tension and in compression.

Bending strain calculations were carried using the spreadsheet programs described in Section 4, and are in accordance with the formulae given in the CoP and in Ref. [11] to determine the magnitude and location of the maximum percent bending measured on the specimen surface, β_{max}.

2.2.3 Results of elastic measurements

The majority of the measurements showed a reasonably linear relationship between maximum bending strain and the applied average axial strain (see example in Fig. 4.) When this is plotted in terms of the maximum percent bending, β_{max}, the highest value of β_{max} (Fig. 5) occurs at low axial strain and falls as the axial strain increases. *Note that the percent bending β_{max} depends also on the orientation of the alignment cell.* The reasons for the observed dependency of bending measurements on specimen orientation were investigated and repeat measurements on a system equipped with a high precision alignment system confirmed that the major cause for such dependency on orientation was mainly due to "bias" in the measuring devices themselves, the alignment cells, as consequences of machining imperfections and errors in the positioning of strain gauges etc.

Figures 6 and 7 show summaries of the inter-laboratory results obtained under elastic loading for the Nimonic 101 and aluminium alloy 6063, respectively. The CoP [7] recommends a 5% limit for the average specimen bending measured at ε_o values of +1000 and -1000 microstrain. As can be seen in Fig. 6, for the Nimonic 101 only 3 out of the 7 laboratories could achieve the recommended level of bending. For the Al 6063 (Fig. 7), no single laboratory could satisfy this 5% bending criterion. One reason for the poor results from the aluminium specimens was thought to be the relatively higher geometrical errors arising from the machining process used to produce them (in terms of concentricity, roundness or parallelism of the surface areas relevant to alignment). Softer materials will always be expected to show higher bending strains due to their lower stiffness.

2.2.4 Results of plastic measurements

Bending measurements and calculations were performed according to Procedure B in the COP at increasing increments of axial strain up to 10,000 microstrain (1% strain) in tension and in compression.

These tests are amongst several novel measurements carried out in the present work. Figure 8 shows a typical example that showed an increase in β_{max} as the specimen deforms plastically. As can be seen, β_{max} reached a minimum value of approximately 1.5% at 3000 and -3000 microstrain (which approximately corresponded to the yield strain of the material tested). Thereafter it increased to a maximum value of about 30% when the axial strain was in compression at 10,000 microstrain (= 1%).

2.2.5 Conclusions from Inter-Laboratory Exercise 1

Analysis of all the results obtained from the above exercise showed that when the readings from the middle set of gauges were excluded the maximum bending in the test remained unchanged in almost every case. In very few cases the maximum bending appeared to occur at the middle of the specimen. This is not, however, consistent with the laws governing bending and it was noted that in all these cases, the difference between the maximum bending strain measured by the middle set of gauges and that determined by the higher of the outer sets of gauges is very small and within the estimated uncertainty of the measurement. It was concluded, therefore, that:

(i) Eight strain gauges are sufficient for measuring the maximum bending strain.

(ii) Measurements in at least 2 diametrically opposite orientations are needed.

(iii) Repeatability of the measurement is very critical for meaningful results.

The above findings were implemented in the simplified procedure adopted in the second inter-laboratory exercise described below.

2.3 Inter-Laboratory Exercise 2

Eight partners were invited to participate in this exercise. In alphabetical order, they were:

CISE Spa, Milan, Italy
ENEL Spa-CRAM, Milan, Italy
INASMET, San Sebastian, Spain
Instron Ltd, High Wycombe, United Kingdom
Materials Engineering & Testing Ltd, Lancaster, United Kingdom
Materials Ireland, Dublin, Ireland
Rolls-Royce plc, Derby, United Kingdom
Rover Group Ltd, Warwick, United Kingdom

Reports were received from 6 organisations. The codes assigned to the relevant partners were chosen at random to preserve anonymity.

Each participant was asked to manufacture their own specimens and make their own arrangements for installing the strain gauges according to the CoP recommendations. The tests involved performing 2 procedures:

- elastic measurements according to Procedure A in the CoP, using an alignment cell made of Nimonic 101, and
- plastic measurements according to Procedure B using a test specimen made of the aluminium alloy 6063.

The elastic measurements involved carrying out 5 repeat runs in each of Orientations 1 and 2. The results were broadly similar to those described above in Section 2.1. Therefore, they are not reported here to avoid repetition.

3. A NEW PROCEDURE FOR THE MEASUREMENT OF MACHINE ALIGNMENT

As described in Section 2.2.3, bending measurements were found to be dependent on the specimen orientation. Further tests using a precision alignment system confirmed that the specimen contribution is more significant than previously thought; in many instances it even exceeded the contribution due to the machine misalignment. A new procedure [11] was developed that separates the contribution from the specimen itself from that due to misalignment of the test machine's load train. The procedure recommends the use of an alignment cell made of a material with high elastic working range and a modulus of elasticity within the range 200-250 GPa (many superalloys and steels are suitable candidates). The cell geometry can be cylindrical or rectangular as appropriate but should fit into the machine grips in the same way as the test specimen. The alignment cell should have at least 8 strain gauges (2 sets of 4) installed at an axial separation, l_g, of 0.75 times the parallel length, l_p (see Fig. 2). It is essential that strain readings are taken in at least 2 diametrically opposite orientations (180^o apart, such as O_1 and O_2 or O_3 and O_4 in Fig. 3). At each orientation, the strain readings should be taken at 5 or more successive levels of axial force, F, or mean axial strain, ε_o, in tension and/or compression as appropriate, according to the mode of loading of the test machine.

The contribution of the test machine misalignment to the total bending measured on the specimen surface can be evaluated by subjecting the specimen to an axial load in one

orientation (e.g. Orientation 1) and recording the strain gauge readings, and by repeating this after rotating the specimen 180° about its vertical axis (i.e. Orientation 2). By rotating the specimen, its bending contribution rotates relative to the machine while the machine's bending component remains stationary. Therefore, averaging the bending strains for any single gauge at 2 diametrically opposite positions gives the bending component due to the specimen at the location of that particular gauge. The machine contribution can be calculated from one half of the difference between the 2 readings. See Ref. [11] for full details.

Reference 11 recommends that the machine alignment be characterised by 1 of 4 classes - Class 2, Class 5, Class 10 and Class 20 - according to the following criteria:

Class	Abs (ε_o) ≤ 1000 με	Abs (ε_o) > 1000 με
2	ε_{bmax} ≤ 20 microstrain	β_{max} ≤ 2 %
5	ε_{bmax} ≤ 50 microstrain	β_{max} ≤ 5 %
10	ε_{bmax} ≤ 100 microstrain	β_{max} ≤ 10 %
20	ε_{bmax} ≤ 200 microstrain	β_{max} ≤ 20 %

The above criterion is shown graphically in Fig. 9. The measurement has proved to be satisfactorily reproducible if well-aligned test systems are used (Fig. 10).

Figure 11 shows a summary of the determined alignment classes for all the test machines used in the 2 inter-laboratory exercises described above in Sections 2.1 and 2.2. As can be seen, 6 out 12 systems conformed to Class 5 alignment.

4. SOFTWARE PROGRAMS FOR ANALYSING STRAIN GAUGE READINGS FOR ALIGNMENT MEASUREMENTS

One of the major targets in this work was to analyse, systematically and reliably, the results of the bending measurement tests. To achieve this, 3 spreadsheets -ALIGNCAL, BENCAL and PLASTICAL - were developed and validated [12]. The calculations run on Microsoft Excel Version 5.0 or higher using input data obtained from alignment or test cells with circular cross-sections and from tests carried out in accordance with the recommendations in Ref. [11]. The main features of these programs are:

- ALIGNCAL separates the bending contribution due to the machine misalignment from that due to errors inherent in the specimen itself and gives the corresponding classification of the machine alignment.

- BENCAL analyses the strain gauge readings and determines the maximum percent bending and other parameters (such as maximum bending strains, the angle θ etc.) according to Procedure A in the CoP.

- PLASTICAL analyses the plastic bending measurements according to Procedure B of the CoP.

All bending measurements produced in this project were analysed using the above-mentioned programs as appropriate.

5. STUDIES OF SPECIFIC PARAMETERS EFFECTING ALIGNMENT MEASUREMENT

5.1 Size of the Alignment Cell

To evaluate the effect of specimen size on bending and alignment measurements, tests were carried out at BMW Rolls-Royce on Nimonic 101 specimens with the same parallel length of 16.2 mm but with a range of different diameters of 4, 6, 7.5 and 10 mm. The tests were performed in accordance with Procedure A of the CoP, in 4 orientations and using the same machine and specimen grips. Figure 12 shows a summary of results in terms of β_{av} from which it can be seen that specimen bending tends to increase slightly as the specimen diameter is decreased. This reflects the effect of the specimen stiffness on the measurements and is analogous to the differences observed when using a specimen made of a hard or a soft material. Figure 13 shows the corresponding machine alignment and from which it can be seen that the measurement can be slightly dependent on the specimen size.

5.2 Variation of Specimen Bending During LCF Tests

This part of the work represents yet another example of the novel measurements carried out in this project. The variation of maximum bending strain during LCF fatigue was assessed using fully reversed stress-controlled tests at ambient temperature with Nimonic 101 strain-gauged specimens. The strain gauge readings were recorded using a fast data acquisition system, capable of scanning at a rate of 25,000 samples per second. The data recorded allowed monitoring of the variation of specimen bending during pre-selected fatigue cycles. Figure 14 shows the results in which the maximum bending gradually increased from approximately 3 to 10% at which point the strain gauges started to fail one by one due to either metal fatigue in the gauges themselves or failure in the bonding adhesive. The machine alignment, which was verified before and after the test, remained unchanged within Class 5. It was concluded, therefore, that in this instance, the observed increase in specimen bending appears to be due to progressive imbalance in the axial strains on the specimen's surface as a result of fatigue cracking in the specimen.

6. BASELINE LCF DATA AT AMBIENT TEMPERATURE

6.1 Specimen Geometry and Preparation

Baseline LCF tests were carried out at NPL on specimens with a nominal diameter of 8.00 ± 0.02 mm, a parallel length of 16.0 mm and transition radii of 30.0 mm (Fig. 15). The specimens were machined from 25 mm diameter blanks by turning followed by grinding between centres according to the instructions shown in Appendix A. Each was numbered such that its position in the source material stock could be identified. The specimens were mechanically polished in the longitudinal direction to produce a typical surface roughness, R_a, of 0.07 µm. The surface finish measurements were performed on a number of specimens chosen randomly. Each measurement involved performing 4 axial runs at 90^o interval rotations about the specimen's axis.

6.2 Test Equipment

The tests were performed on a servo-electric, 2-column test machine type Instron 8562 with a frame capacity of 250 kN. The machine was equipped with a 100 kN load cell and 8500 PLUS controller. The load cell was calibrated to Class 1 according to BS EN 10002-2: 1992. Two types of single-sided extensometers were used to measure the extension depending on the test temperature. Both extensometers were calibrated to Class 0.5 according to BS EN 10002-4:1995. For the tests at ambient temperature, a clip gauge extensometer, manufactured by Instron, was used. It had a 12.5 mm gauge length and an axial deformation range of ± 2.5 mm.

The machine was located in a temperature-controlled environment that was kept at 21^{o}C ± 2^{o} and a relative humidity RH of 50% ± 10%. The machine was equipped with an alignment fixture manufactured by Instron. The machine alignment, which was measured before and after each test using a Nimonic 101 alignment cell, was determined using the program ALIGNCAL. An essential requirement before commencing any test was that the machine alignment satisfies Class 5. This was achieved using a then newly introduced grip system, shown schematically in Fig. 16. The vast majority of tests were completed while the machine remained within Class 5; but in about a quarter of the tests (see Fig. 17) it was noted that the alignment deteriorated slightly during the test to Class 10 and, in one case, to Class 20. Such changes in alignment during the test were not considered significant enough to invalidate these tests.

During the fatigue tests the test system was controlled by computer, which also had the task of collecting and digitally processing the data. The software used was Instron LCF Version 2.10. Approximately 200 data points were collected per loop.

6.3 Test Conditions

The vast majority of these tests were strain-controlled with fully reversed triangular waveforms and a strain rate of 2.0 $\times 10^{-3}$ s^{-1} (=12.0%/minute). The failure criterion in these tests was the number of cycles to achieve a 25% decrease in the maximum force over the intermediate part of the test (see Fig. 8 in ISO DIS 12106 [8] for a graphical representation). The total strain range values were chosen to produce fatigue lives typically in the range of 10^2 to 10^5 cycles. After each test, the specimen was examined using a low magnification optical microscope to determine the most likely location of the major crack initiation site that led to eventual failure.

Four tests were carried out in fully reversed stress-controlled mode ($\Delta\sigma$ = 1200 MPa) with sinusoidal waves and at a frequency of 1 Hz. The failure criterion in these tests was complete fracture of the specimen.

As can be seen in the examples in Fig. 18, at ambient temperature the cyclic deformation behaviour showed a slight softening in the first few cycles at the beginning of the test, which was followed by modest cyclic hardening. However, the overall behaviour can be described as relatively stable.

Table 4 gives a summary of the test results, where the stress and strain values shown are those determined from the hysteresis loop nearest to mid-life. Caution should be

exercised in interpreting the information on the location of failure on the specimen's surface as in most cases the specimen had many small cracks all around the surface and it was difficult to decide with certainty the exact location of the major crack initiation site. Multiple and uniform cracking around and along the specimen surface is a good indication of the high level of alignment achieved in these tests. A significant number of tests appeared to have failed outside the 12.5 mm gauge length (c_o = ± 6.25 mm) but these were still considered valid and included in the analysis. It is important to report that no specimens appear to have failed where the extensometer probes were located. Figure 19 shows the fatigue life curves and Table 5 includes the corresponding best-fit equations in terms of the strain range components $\Delta\varepsilon_t$, $\Delta\varepsilon_p$ and $\Delta\varepsilon_e$.

7. BASELINE LCF DATA AT 850^{O}C

Baseline elevated temperature LCF tests were conducted at NPL using the same material, specimen and test facility described above. The specimen was heated using a 3 zone split furnace and the temperature was monitored by 2 type R platinum-rhodium alloy wire thermocouples attached to the specimen surface at both ends of its parallel length. The specimen was heated to the test temperature at a rate of approximately 15 ^{o}C/minute and was held at temperature for about 60 minutes before measuring Young's modulus and starting the test. The thermocouples were calibrated against an NPL standard reference thermocouple. At a nominal temperature of 850 ^{o}C, the error in the indicated reading was typically within ±0.5 ^{o}C. The temperature profile along the specimen's parallel length was determined using a dummy specimen with 3 thermocouples attached to its surface, one at the centre and one at each end of the gauge length. The temperature variation was found to be within ±1.4 ^{o}C, being hotter in the middle. During each test, the temperature was recorded at regular intervals and the indicated thermocouple readings were maintained to within ±2.0 ^{o}C from the target value.

The specimen's axial deformation was measured using a single-sided extensometer, type MTS 832-41F-11, which had a 12.0 mm gauge length and was fitted with quartz rods. The extensometer was calibrated to Class 0.5 specification according to EN 10002-4:1994.

Most of the tests were carried out at a nominal temperature of 850 ^{o}C but some were at 825 ^{o}C or 875 ^{o}C. The tests were performed at different levels of total-strain control to produce fatigue lives typically within the range 10^2 to 2.0×10^4 cycles. The strain rate was kept constant at 1.0×10^{-3} s^{-1} (=6.0 % per minute).

Table 6 summarises the test results at 850 ^{o}C, where the stress and strain values shown are those determined from the hysteresis loop nearest to mid-life. In these tests, the deformation behaviour was characterised by classic strain softening - Fig. 20. The rate of softening falls rapidly in the initial part of the test until it reaches a minimum value then gradually increases towards the final failure stage with the customary increasing drop in load. Figure 21 shows the resultant fatigue life curves at 850 ^{o}C and the corresponding mathematical equations fitted to the resultant lifetime curves are included in Table 5.

The results of the LCF tests carried out at 825°C and 875°C are included in Tables 7a and 7b, respectively. These temperatures were chosen to determine the sensitivity of the material to ± 25°C temperature variations from the 850°C used previously. The 25°C interval between the nominal temperature and the upper and lower temperature levels was chosen on the basis that it is about 5 times the estimated uncertainty in the temperature measurement at 850°C. As can be seen in Fig. 22, the sensitivity of fatigue life to test temperature appears to follow a reasonably linear relationship, which is used in the uncertainty analysis in Section 10.

8. INTERCOMPARISON EXERCISE ON LCF OF NIMONIC 101 AT AMBIENT TEMPERATURE

8.1 Participating Laboratories

The following 6 laboratories carried out the tests included in this part of the work:

BMW Rolls-Royce AeroEngines (BRR), Germany
Consiglio Nazionale delle Ricerche (CNR - TEMPE), Italy
National Physical Laboratory (NPL), United Kingdom
Swedish Institute for Metals Research (SIMR), Sweden
TNO Institute of Industrial Technology (TNO), The Netherlands
VTT Manufacturing Technology (VTT), Finland

The codes adopted in this part of the work were chosen randomly to preserve anonymity.

8.2 Specimen Geometry and Preparation

All the specimens used in this part of the work were machined and polished at one organisation, NPL, following the same specifications and machining route described in Appendix A. The dimensions of the cylindrical parallel portions were all identical, 8.00 ± 0.02 mm in diameter with a 16.0 mm parallel length and transition radii of 30.0 mm. The grip ends (and therefore the overall lengths) varied according to the participants' specific gripping requirements. Figure 24 shows the specimen geometries used. Surface finish measurements were performed on at least 1 specimen selected at random from each group and the results confirmed that the surface finish was indeed consistent with those reported previously in Section 6.1.

8.3 Test Equipment, Conditions and Results

Table 8 shows details of the test equipment used. All participants utilised digitally controlled systems. It was required that Class 5 machine alignment be used but 2 participants, C and E, had Class 20 and 10, respectively. Each participating laboratory carried out 6 tests, 3 in strain control with a nominal total strain range of 1.0% and 3 in stress control with a nominal stress range of 1200 MPa. Table 9 presents a summary of the test results.

8.4 Uncertainties Evaluations

8.4.1 Uncertainty Evaluation for Young's Modulus Measurements

Uncertainty evaluation procedures for LCF testing were developed in the present project and included in Ref. [13]. Table 10 presents the uncertainty budget for Young's modulus, from which it can be seen that the estimated uncertainty is ± 5.5%. This is applicable to the tests at ambient and elevated temperature and, as can be seen in Figs. 23 and 25, the experimental data agrees reasonably well with the estimated 95% probability band. Achieving agreement in modulus results to within ±5% of the mean value (Fig. 25) reflects the high standard of the test procedures used in this work and is now *an ISO requirement* [8].

8.4.2 Uncertainty Evaluation for LCF Life in Strain-controlled Tests

The calculations for the uncertainty in fatigue life for the strain-controlled tests at ambient temperature are shown in Table 11 (and graphically in Fig. 26). Good agreement was achieved in the data sets for labs A, B & D that had Class 5 alignment. The results for Lab E (alignment Class 10) and Lab C are somewhat lower relative to the other data sets. This has emphasised the need for satisfying the alignment requirements as all other variables in these tests were reasonably eliminated.

8.4.2 Uncertainty Evaluation for LCF Life in Stress-controlled Tests

The calculations for the uncertainty in fatigue life for the stress-controlled tests at ambient temperature are shown in Table 12 (and graphically in Fig. 27). The agreement in this case seemed better than in the strain-controlled tests, which may indicate that stress-controlled tests are less prone to specimen bending effects. As can be seen, all the data sets including those with alignment Class 10 and 20 fall within the predicted uncertainty band. The scatter factor was 1.53, well within the target of less than 5.

9. SYSTEMATIC STUDY OF EFFECTS OF SUPERIMPOSED BENDING ON LCF BEHAVIOUR OF NIMONIC 101 AT 850^{O}C

Novel LCF tests with predetermined levels of superimposed maximum percent bending were carried out (see Scholz, Darmstadt University, [14]) to establish the effects of specimen bending on fatigue life. The percent bending used, β_{1000}, which corresponds to an axial strain, ε_o, of 1000 microstrain, had nominal values of 2, 20 or 40%. These predetermined superimposed bending levels were achieved by using a special alignment fixture made by Schenck that allowed well-controlled lateral displacements of one end of the specimen to be introduced relative to the other. The extension was measured by a side-entry, single extensometer placed at right angles to the direction of the maximum bending strain on the specimen. All the tests were performed on the same machine under the same testing conditions with specimens made from the same batch of Nimonic 101 at a nominal temperature of 850^{o}C. To enable the precise control of the alignment, a specially designed specimen was developed with its ends shrink fitted into extension bars made of Nimonic 80A. A total of 18 strain-controlled tests were carried out, 9 each at $\Delta\varepsilon_t$ of 1.1% and 0.5%. Every specimen was strain-gauged with 12 gauges and bending measurements were performed at ambient temperature. After the bending

measurement, the specimen was heated to about 300°C and the strain gauges and adhesive carefully removed.

The test results are summarised in Table 13 and shown graphically in Fig. 28. For the tests with $\Delta\varepsilon_t$ of 1.1%, the fatigue life appears to fall progressively as β_{1000} is increased. On the other hand, the fatigue life for the lower strain range of $\Delta\varepsilon_t$ of 0.5% remains practically unchanged.

10. VAMAS MINI INTERCOMPARISON LCF TESTS ON NIMONIC 101 AT 850°C

10.1 Objectives

The aim in this part of the work was to apply the uncertainty analysis and new improved procedures developed in this work to a small data set. Only three laboratories were involved in this part of the work, NPL, University of Darmstadt (IFW) and the National Research Institute for Metals (NRIM). All the tests were conducted on the same batch of material, at the same nominal temperature of 850 °C, under identical test conditions and with the same requirement of machine alignment level of Class 5. It must be pointed out however, that there were significant variations in other aspects of the test details including the specimen geometry and surface preparation procedures, the method of heating and temperature measurement. Note also that in this exercise each laboratory machined its own specimens, unlike the inter-comparison exercise at ambient temperature described in Section 8. It was agreed not to attempt to harmonise all the test details to maintain some elements of variability in the testing practices to reflect what happens in day-to-day practices in industry and research. Table 14 includes a summary of information on the testing equipment used in this part of the work.

10.2 Test Conditions and Results

The principal test conditions were:

Total strain range	1.2% and 0.5%
Strain ratio	-1
Waveform	triangular
Strain rate	1×10^{-3} s^{-1} (= 6.0 % per minute)
Nominal test temperature	850°C
Direction of first loading	tension
Definition of failure	N_{25}
Number of repeat tests	3 (NRIM performed 4 tests at $\Delta\varepsilon_t$ = 0.5% and 6 tests at 1.2%)

The IFW and NRIM data are summarised in Tables 15 and 16, respectively. Note that the IFW data are those described in Section 9 at 2% specimen bending. The NPL data are those described in Section 7. The inter-comparison results for Young's modulus, fatigue life at total strain range values of $\Delta\varepsilon_t$ of 1.2% and 0.5% are shown graphically in Figs. 29 to 31, respectively.

10.3 Discussion and Uncertainties Evaluations

Figure 29 shows that almost all the experimental results for Young's modulus are within the estimated expanded uncertainty of ±5.5%. This again reflects the high standard of testing procedures used. Tables 17 and 18 show the estimated testing uncertainty calculations for fatigue life at 850°C for total strain range values of $\Delta\varepsilon_t$ = 1.2% and 0.5%, respectively. These are also included in Figs. 30 and 31. The calculations were based on the following assumptions:

1 - the testing machines are aligned to Class 5,

2 - no errors in the control of the nominal total strain range,

3 - strain measurement errors (including errors due to resetting the extensometer before starting the test) are within ±1.5%,

4 - temperature measurement errors (from all sources) are within ± 4°C, and

5 - no variability exists in specimen size, residual stresses due to machining and surface finish, and the method of determining N_f.

The results in Figs. 30 and 31 show that there *were* systematic (lab-to-lab) variations in the fatigue life results. Note that in Fig. 30, IFW used a lower strain range, 1.1% instead of the 1.2 % used by both NPL and NRIM. The NPL data appear to be consistently higher than those for IFW and NIRM and a detailed examination of the data indicated that the most probable reason was due to systematic errors in temperature measurement and control (note that all systems complied with Class 5 alignment). As can be seen from the NPL results at 825, 850 and 875 °C, the modulus of elasticity remained almost unchanged within this temperature range. If the temperature changes, the plastic strain will also change, since in these tests the total strain range was the control variable.

Figure 32 shows a reasonable representation of fatigue life in terms of the plastic strain range for all the tests performed by NPL, IFW and NIRM, within the range 825 °C to 875 °C. This confirms the hypothesis that the observed lab-to-lab systematic variability in fatigue life may be attributed to the different methods used to measure and control the temperature.

It is encouraging, however, that despite the systematic variations discussed above, the highest inter-laboratory scatter factor was still well within the initial aimed target of less than 5.

CONCLUSIONS

From the above reported work the following main conclusions were made:

1 The project has achieved all its objectives. These include identifying ways in which the variability in inter-laboratory fatigue life data can be maintained to a factor of less than 5,

2 A new procedure has been produced and validated for verifying the alignment of uniaxial test machines. The procedure incorporates an alignment classification system

3 Three software programs called AlignCal, BenCal and PlastiCal, were developed and validated for analysing systematically and reliably the strain gauge readings used in measuring specimen bending and verifying machine alignment,

4 It is recommended that Class 5 alignment is used as the standard requirement for quality fatigue testing,

5 For tests carried out on machines with an alignment Class 5, the inter-laboratory scatter in fatigue life is much reduced compared with similar previous exercises,

6 The inter-laboratory scatter in fatigue life at ambient temperature with an alignment Class 5 was within a scatter factor, N_{fmax}/N_{fmin}, of 1.5. This is well within the target value of a factor of 5,

7 The inter-laboratory scatter in fatigue life at 850 ^{o}C exceeded the estimated testing uncertainties based on the baseline date, but was still well within the target value of a factor of 5,

8 Stress-controlled tests are less prone to specimen bending effects than strain-controlled tests,

9 Specimen bending tends to reduce fatigue life in strain-controlled Nimonic 101 at 850 ^{o}C,

10 Fatigue life curves in terms of plastic strain range are relatively insensitive to small changes in temperature,

11 Two sets of 4 strain gauges are sufficient to measure the specimen bending or to verify the machine alignment,

12 Elastic bending measurements in at least 2 opposite orientations are essential to characterise the machine alignment,

13 Percent bending increases significantly as the specimen is deformed plastically,

14 Specimen bending under plastic deformation cannot be predicted from or correlated to the elastic measurements,

15 Elastic bending measurements do not necessarily characterise the quality of any test that involves plastic deformation, and

16 Alignment cells should be made of relatively hard monolithic metallic materials. Soft materials such as aluminium alloy 6063 are not recommended.

ACKNOWLEDGEMENTS

The tests reported in this publication were performed within Project MAT1-CT94-0079, *'Quantifying Data Uncertainties and the Validation of a Code of Practice for the Measurements of Bending in Uniaxial Fatigue Test Pieces'*. The project was partially funded by the Commission of European Communities through the Standards, Measurement and Testing programme.

The author gratefully acknowledges the invaluable contributions made by his European and VAMAS Partners. Many thanks are also due to Dr Carlos Saraiva-Martins for his continued guidance and encouragement and for approving this publication. The author is indebted to Mr Terry Gorley for reading this manuscript.

This report was produced with support from the UK Department of Trade and Industry as part of a programme of underpinning research on materials measurements.

REFERENCES

1. F A Kandil, "*Quantifying Data Uncertainties and the Validation of a Code of Practice for the Measurement of Bending in Uniaxial Fatigue Test Pieces*", Final Report, Project MAT1-CT94-0079, NPL, October 1999.

2. G B Thomas and R K Varma, "*Evaluation of low cycle fatigue test data in the BCR/VAMAS inter-comparison programme*", Report EUR 14105 EN, ISSN 1018-5593, Commission of the European Communities, 1993.

3. F A Kandil, and B F Dyson, '*Systematic study of effects of load misalignment in uniaxial low cycle fatigue testing at high temperatures*', NPL Report DMM(A)27, National Physical Laboratory, UK, July 1991.

4. F A Kandil, and B F Dyson, '*The influence of load misalignment during uniaxial low cycle fatigue testing. I- Modelling*', *Fatigue Fract. Engng. Mater. Struct.* 16, No. 5, pp. 509-27, 1993.

5. F A Kandil, and B F Dyson, '*The influence of load misalignment during uniaxial low cycle fatigue testing. II- Applications*', ibid, 16, No. 5, pp. 529-37, 1993.

6. F A Kandil, and B F Dyson, '*Prediction of uncertainties in low cycle fatigue data*', Conf. Proc. Creep and Fracture of Engineering Materials and Structures, Swansea, UK, 28 March - 2 April 1993, Edited by B Wilshire and R W Evans, pp 517-25, The Institute of Materials, London, 1993.

7. F A Kandil, "*Measurement of Bending in Uniaxial Low Cycle Fatigue Testing*", Measurement Good Practice Guide No. 1, NPL, ISSN 1368-6550, March 1998. Initially published as "*Code of Practice for the Measurement of Bending in Uniaxial Low Cycle Fatigue Testing*", Best Practice in Measurement Series, NPL, ISBN 0 946754-16-0, MMS 001:1995.

8. ISO DIS 12106, "*Metallic Materials - Fatigue Testing - Axial Strain-controlled Method*"

9. Pr EN3874 "*Constant Amplitude Load-controlled Low Cycle Fatigue Testing*", AECMA Aerospace Series - Test Methods for Metallic Materials, March 1998.

10. Pr EN1988, "*Constant Amplitude Strain-controlled Low Cycle Fatigue Testing*", AECMA Aerospace Series - Test Methods for Metallic Materials, March 1998.

11. F A Kandil, "*Verification of Alignment of Uniaxial Test Systems*", VAMAS Report No. 42, ISSN 1016-2186, National Physical Laboratory, February 2003.

12. F A Kandil, "*AlignCal, BenCal and PlastiCal - The NPL Software Package for Alignment and Bending Measurements Calculations*", V14, National Physical Laboratory, September 1998.

13. F A Kandil, "*The Determination of Uncertainties in Low Cycle Fatigue Testing*", UNCERT CoP 02:2000, in "Manual of Codes of Practice for the Determination of Uncertainties in Mechanical Tests on Metallic Materials", F A Kandil et al Eds. ISBN 0-946754-41-1, Issue 1, September 2000, National Physical Laboratory.

14. A Scholz, "*Influence of Bending on Low Cycle Fatigue Life of Cylindrical Test Pieces*", Institute of Materials Technology, Darmstadt University of Technology, in Proc. of 21st "Vortragsveranstaltung, "Langzeitverhalten warmfester Stähle and Hochtemperaturwerkstoffe" der Arbeitsgemeinschaften warmfester Stähle und Hochtemperaturwerkstoffe, Düsseldorf, P. 121/32, 27 November 1998.

Table 1. Basic properties of Nimonic 101 alloy as supplied by Wiggin Alloys Ltd (UK)
(Cast Identification Number HLN877)

Mechanical composition in weight percent (Manufacturer's data)

C	Si	Mn	S	Al	Co	Cr	Cu	Fe	Mo	Nb	Ta	Ti	V	W	Zr	Trace elements in ppm											Ni
																Ag	As	B	Bi	Pb	Sb	Sn	Te	Tl	Zn	Hg	
0.053	0.08	0.07	0.001	1.41	19.4	24.25	0.01	0.18	1.45	0.91	0.05	3.01	0.01	0.05	0.054	0.1	10	131	0.1	0.1	1.0	7.0	1.0	0.2	1.0	5	Bal

Form Extruded bars, 25 mm diameter.

Final stage heat treatment 1120°C, 1 h, air cooled; 850°C, 16 h, air cooled

Grain size 75 - 110 micrometers (ASTM No 3.5 - 4.5)

Mechanical test results (Manufacturer's data)

PROPERTY	UNIT	22°C		750°C		850°C	
		BAR 3A	BAR 3B	BAR 3A	BAR 3B	BAR 3A	BAR 3B
0.1% Proof stress	MPa	758					
0.2% Proof stress	MPa	774	793	698	680	505	524
Tensile strength (R_m)	MPa	1206	1234	933	931	635	657
Elongation (on 5.65 /√Area)	%	17.9	22.9	20.5	23.1	20.5	20.1
Young's modulus (E)	GPa	234	226	179		158	
Hardness H_{v30}	Vickers	360					

Table 2. Testing machines used in Inter-Laboratory Exercise 1

Partner	Machine	Load capacity (+/- kN)	Class of load cell	Alignment method	Alignment cell dimensions in mm		
					d	l_p	l_g
A	Instron 8562	100	1	Instron alignment fixture + Instron AlignPro software	7.50 ±0.01	16.2	12.0
B	Instron 8562	100	1	Instron alignment fixture + Instron AlignPro software	7.50 ±0.02	16.2	12.0
C	MTS 810	250	1	MTS 609 alignment fixture	7.50 ±0.01	16.2	12.0
D	Schenck	100	1	Dial gauge + strain-gauged specimen	8.00 ±0.01	19.6	14.7
E	Instron 1380	30	1	Strain-gauged specimen	7.50 ±0.01	16.2	12.0
F	MTS 311-1	250	1	Wood's metal grips (self-aligning)	7.50 ±0.01	16.2	12.0
G	MTS 810	100	1	MTS Alignment fixture	7.50 ±0.01	16.2	12.0

Table 3. Details of strain gauges used in Inter-Laboratory Exercise 1

Partner	Specimen material	Specimen code	Strain gauge						Adhesive	
			Manufacturer	Type	Length, mm	Grid width, mm	Electrical resistance	Gauge factor	Type	Coating
A	Nimonic 101	AVA01	MM[1]	EA-06-062AQ-350	1.57	1.57	350	2.09	M bond 610	M coat C
	Nimonic 101	AVA02	MM	EA-06-062AQ-350	1.57	1.57	350	2.09	M bond 610	M coat C
	Al 6063	AVD01	MM	EA-13-062AQ-350	1.57	1.57	350	2.12	M bond 600	M coat C
	Al 6063	AVD02	MM	EA-13-062AQ-350	1.57	1.57	350	2.12	M bond 600	M coat C
B	Nimonic 101	AVA33	MM	EA-06-062AQ-350	1.57	1.57	350	2.09	M bond 610	M coat C
	Nimonic 101	AVA34	MM	EA-06-062AQ-350	1.57	1.57	350	2.09	M bond 610	M coat C
	Al 6063	AVD30	MM	EA-13-062AQ-350	1.57	1.57	350	2.14	M bond 600	M coat C
C	Nimonic 101	AVA11	MM	EA-06-062AQ-350	1.57	1.57	350	2.09	M bond 610	M coat C
	Nimonic 101	AVA12	MM	EA-06-062AQ-350	1.57	1.57	350	2.09	M bond 610	M coat C
	Al 6063	AVD11	MM	EA-13-062AQ-350	1.57	1.57	350	2.12	M bond 600	M coat C
	Al 6063	AVD12	MM	EA-13-062AQ-350	1.57	1.57	350	2.12	M bond 600	M coat C
D	Nimonic 101	AVA03	HBM[2]	LY61 1.5/120	1.5	1.2	120	1.86	Z70	PU120
	Al 6063	AVD08	HBM	LY63 1.5/120	1.5	1.2	120	1.86	Z70	PU120
E	Nimonic 101	AVA15	MM	EA-06-062AQ-350	1.57	1.57	350	2.09	M bond 610	M coat C
	Nimonic 101	AVA14	MM	EA-06-062AQ-350	1.57	1.57	350	2.09	M bond 610	M coat C
	Al 6063	AVD29	MM	EA-13-062AQ-350	1.57	1.57	350	2.12	M bond 600	M coat C
	Al 6063	AVD28	MM	EA-13-062AQ-350	1.57	1.57	350	2.12	M bond 600	M coat C
F	Nimonic 101	AVA16	MM	EA-06-062AQ-350	1.57	1.57	350	2.09	M bond 610	M coat C
	Nimonic 101	AVA15	MM	EA-06-062AQ-350	1.57	1.57	350	2.09	M bond 610	M coat C
	Al 6063	AVD09	MM	EA-13-062AQ-350	1.57	1.57	350	2.12	M bond 600	M coat C
	Al 6063	AVD10	MM	EA-13-062AQ-350	1.57	1.57	350	2.12	M bond 600	M coat C
G	Nimonic 101	AVA09	MM	EA-06-062AQ-350	1.57	1.57	350	2.09	M bond 610	M coat C
	Nimonic 101	AVA10	MM	EA-06-062AQ-350	1.57	1.57	350	2.09	M bond 610	M coat C
	Al 6063	AVD13	MM	EA-13-062AQ-350	1.57	1.57	350	2.12	M bond 600	M coat C
	Al 6063	AVD14	MM	EA-13-062AQ-350	1.57	1.57	350	2.12	M bond 600	M coat C

1 MM = Micro Measurements
2 HBM = Hottinger Baldwin Meβtechnik

Table 4. Summary of LCF tests on Nimonic 101 at ambient temperature (baseline data)

(a) Strain-controlled tests

Specimen ID	Values at mid-life: Strain range, % $\Delta\varepsilon_t$	$\Delta\varepsilon_p$	$\Delta\varepsilon_e$	Stress, MPa σ_{max}	σ_{min}	$\Delta\sigma$	σ_m	Frequency Hz	Modulus E_0, GPa	Modulus $E_{1/4}$, GPa	N_{25}	Location of failure: c, mm	c_0, mm	θ_c, degrees	Remarks
AVB11	2.998	1.811	1.187	1083.28	-1125.68	2208.96	-21.20	0.033	218.2	218.2	124	32.06	8.38	20	(2)
AVB50	3.010	1.817	1.193	1087.41	-1126.18	2213.59	-19.39	0.033	217.9	218.3	200	15.62	-8.06	250	(2)
AVB12	1.993	0.939	1.054	992.46	-1067.89	2060.35	-37.72	0.050	216.8	219.4	1115	16.7	-6.98	270	(2)
AVB48	2.017	0.955	1.062	1001.76	-1034.59	2036.35	-16.42	0.050	207.6	218.1	1301	16.67	-7.01	260	(2)
AVB47	1.509	0.534	0.975	939.34	-982.30	1921.64	-21.48	0.033	213.1	214.3	2392	25.27	1.59	270	
AVB13	1.496	0.516	0.980	913.06	-1034.90	1947.96	-60.92	0.067	223.1	218.1	2590	20.6	-3.08	270	
AVB31	1.002	0.166	0.836	852.66	-885.60	1738.26	-16.47	0.100	205.7	219.9	7853	NA	NA	NA	NA
AVB43	1.012	0.171	0.841	872.58	-868.69	1741.27	1.94	0.100	220.8	219.3	8580	19.72	-3.96	250	
AVB45	0.999	0.158	0.841	812.91	-919.93	1732.84	-53.51	0.100	214.2	216.9	9112	30.47	6.79	10	(2)
AVB42	0.998	0.160	0.838	841.04	-886.16	1727.20	-22.56	0.100	219.2	216.3	9125	31.99	8.31	315	(2)
AVB49	0.813	0.065	0.748	766.53	-835.01	1601.54	-34.24	0.125	207.6	218.0	15433	18.25	-5.43	270	
AVB14	0.799	0.057	0.742	745.39	-833.54	1578.93	-44.08	0.125	215.1	218.0	16365	26.42	2.74	120	
AVB35	0.599	0.004	0.595	536.56	-788.53	1325.09	-125.99	0.167	223.6	219.4	70700	M	M	M	
AVB15	0.599	0.006	0.593	378.29	-915.98	1294.27	-268.85	0.167	215.4	217.7	104935	M	M	M	

(b) Stress-controlled tests

Specimen ID	Values at mid-life: Strain range, % $\Delta\varepsilon_t$	$\Delta\varepsilon_p$	$\Delta\varepsilon_e$	Stress, MPa σ_{max}	σ_{min}	$\Delta\sigma$	σ_m	Frequency Hz	Modulus E_0, GPa	Modulus $E_{1/4}$, GPa	N_{25}	Location of failure: c, mm	c_0, mm	θ_c, degrees	Remarks
AVB44	NA	NA	NA	600.0	-600.0	1200.0	0.0	1.0	NR	NR	70533	20.36	-3.32	270	
AVB38	NA	NA	NA	600.0	-600.0	1200.0	0.0	1.0	NR	NR	84428	20.15	-3.53	170	
AVB37	NA	NA	NA	600.0	-600.0	1200.0	0.0	1.0	NR	NR	89123	24.55	0.87	315	
AVB40	NA	NA	NA	600.0	-600.0	1200.0	0.0	1.0	NR	NR	109964	23.7	0.02	240	

M Multiple cracking
NA Not applicable
NR Not reported
(1) Failure outside the gauge length
(2) Failure outside the parallel length

Table 5. Low cycle fatigue life equations for strain-controlled tests on Nimonic 101 (baseline data)

Test temperature	Strain parameter	Life equation [1)]	R or R^2
21°C	Total	$\log(\Delta\varepsilon_t) = -1.14206 + 1.79471\times[\log(N_f)] - 0.60538\times[\log(N_f)]^2 + 0.05662\times[\log(N_f)]^3$	$R^2 = 0.99815$
	Plastic	$\log(\Delta\varepsilon_p) = 3.13138 - 1.01056\times[\log(N_f)]$	$R = -0.97556$
	Elastic	$\log(\Delta\varepsilon_e) = 0.42954 - 0.13009\times[\log(N_f)]$	$R = -0.98941$
850 °C	Total	$\log(\Delta\varepsilon_t) = 1.22344 - 0.5942\times[\log(N_f)] + 0.05511\times[\log(N_f)]^2$	$R^2 = 0.99662$
	Plastic	$\log(\Delta\varepsilon_p) = 1.72127 - 0.82867\times[\log(N_f)]$	$R = -0.99121$
	Elastic	$\log(\Delta\varepsilon_e) = 0.16834 - 0.11478\times[\log(N_f)]$	$R = -0.99045$

1) Stain ranges in percent

Table 6. Summary of strain-controlled LCF tests on Nimonic 101 at 850^{0}C (baseline data)

	Values at mid-life							Frequency	Modulus E_0,	Modulus $E_{1/4}$,	N_{25}	Location of failure			Remarks
	Strain range, %			Stress, MPa											
Specimen ID	$\Delta\varepsilon_t$	$\Delta\varepsilon_p$	$\Delta\varepsilon_e$	σ_{max}	σ_{min}	$\Delta\sigma$	σ_m	Hz	GPa	GPa		c, mm	c_0, mm	θ_c, degrees	
AVB28	2.007	1.118	0.889	606.35	-623.43	1229.78	-8.54	0.025	163.9	161.7	73	23.54	0.570	20	
AVB109	1.210	0.414	0.796	588.80	-582.52	1171.32	3.14	0.042	163.8	166.6	291	22.966	-0.004	0	
AVB20	1.211	0.436	0.775	577.05	-583.19	1160.24	-3.07	0.042	162.0	163.8	309	19.607	-3.363	45	
AVB19	1.213	0.460	0.753	546.15	-549.88	1096.03	-1.87	0.042	154.2	151.4	315	21.234	-1.736	270	
AVB17	1.215	0.474	0.741	507.12	-524.37	1031.49	-8.63	0.042	153.0	152.5	365	24.075	1.105	315	
AVB21	1.006	0.298	0.708	553.87	-539.80	1093.67	7.04	0.050	160.1	159.3	602	20.813	-2.157	315	
AVB112	1.001	0.261	0.740	551.39	-550.09	1101.48	0.65	0.050	161.3	162.2	606	21.246	-1.724	180	
AVB24	1.002	0.332	0.670	533.90	-520.49	1054.39	6.70	0.050	162.4	159.9	645	24.978	2.008	100	
AVB26	0.801	0.161	0.640	528.06	-513.93	1041.99	7.07	0.063	161.9	166.2	1085	17.968	-5.002	255	
AVB111	0.698	0.074	0.624	523.09	-487.17	1010.26	17.96	0.071	164.9	162.2	2506	M	M	M	
AVB22	0.596	0.060	0.536	481.03	-441.11	922.14	19.96	0.083	161.0	162.8	4694	18.937	-4.033	90	
AVB27	0.495	0.016	0.479	411.72	-363.84	775.56	23.94	0.100	162.6	163.7	17912	M	M	M	
AVB18	0.492	0.010	0.482	412.19	-346.95	759.14	32.62	0.100	154.0	154.7	18481	32.366	9.396	315	(1)
AVB25	0.495	0.017	0.478	409.81	-363.86	773.67	22.98	0.100	162.7	160.9	18643	14.532	-8.438	45	(1)

M Multiple cracking
(1) Failure outside the parallel length

Table 7. Summary of strain-controlled LCF tests on Nimonic 101 at 825°C and 875°C (baseline data)

(a) Tests at 825°C

	Values at mid-life							Frequency	Modulus E_0,	Modulus $E_{1/4}$,	N_{25}	Location of failure			Remarks
	Strain range, %			Stress, MPa											
Specimen ID	$\Delta\varepsilon_t$	$\Delta\varepsilon_p$	$\Delta\varepsilon_e$	σ_{max}	σ_{min}	$\Delta\sigma$	σ_m	Hz	GPa	GPa		c, mm	c_0, mm	θ_c, degrees	
AVB29	1.205	0.372	0.833	641.78	-645.79	1287.57	-2.01	0.042	164.9	166.5	397	25.145	2.175	30	
AVB30	1.205	0.371	0.834	645.51	-644.08	1289.59	0.71	0.042	164.8	167.4	421	20.49	-2.480	10	
AVB74	0.495	0.013	0.482	441.92	-364.18	806.10	38.87	0.100	166.0	167.9	31062	31.41	8.440	180	(1)

(b) Tests at 875°C

	Values at mid-life							Frequency	Modulus E_0,	Modulus $E_{1/4}$,	N_{25}	Location of failure			Remarks
	Strain range, %			Stress, MPa											
Specimen ID	$\Delta\varepsilon_t$	$\Delta\varepsilon_p$	$\Delta\varepsilon_e$	σ_{max}	σ_{min}	$\Delta\sigma$	σ_m	Hz	GPa	GPa		c, mm	c_0, mm	θ_c, degrees	
AVB115	1.208	0.509	0.699	511.57	-503.70	1015.27	3.94	0.042	161.5	160.8	235	20.269	-2.701	80	
AVB116	1.206	0.493	0.713	512.14	-507.21	1019.34	2.47	0.042	155.2	154.4	236	20.121	-2.849	170	
AVB117	0.495	0.027	0.468	406.15	-329.44	735.59	38.36	0.100	157.8	158.3	7624	24.392	1.422	315	

M Multiple cracking
(1) Failure outside the parallel length

Table 8. Test equipment used in the inter-laboratory LCF programme at ambient temperature

Laboratory	Test machine	Frame capacity (+/- kN)	Load cell capacity (+/- kN)	Class of machine [1]	Extensometer type	Extensometer details		
						GL, mm	Range, ± mm	Class [2]
A	Instron 8562 (2 columns)	250	100	1	Instron 2620-602	12.5	2.5	0.5
B	Instron 8562 (2 columns)	250	100	0.5	MTS 632.51F-04	12.0	NR	NR
C	MTS 810 (2 columns)	250	50	0.5 [3]	MTS 632.50C-04	12.0	0.5	B2 [4]
D	MTS 311.1 (4 columns)	250	250	1	MTS 632.11C-20 NR.604	15.0	0.15	0.5
E	MTS 810 (2 columns)	250	100	1	MTS 632.26C	8.0	0.16	0.5

Laboratory	Alignment Class		Alignment method	Ambient temperature, °C
	Before test series	After test series		
A	5	5	Instron alignment fixture	21 ± 2
B	5	5	Instron alignment fixture	NR
C	NR	20	MTS alignment fixture	20
D	NA (Assumed to comply with Class 5)	NA (Assumed to comply with Class 5)	Wood's metal pot grips (Self-aligning)	19 - 20
E	NR	10	MTS alignment fixture	22

1) According to EN 10002-2, unless stated otherwise.
2) According to EN 10002-4, unless stated otherwise.
3) According to ISO R 147.
4) According to ASTM E83.
NA Not applicable.
NR Not reported.

Table 9. Summary of inter-laboratory LCF data on Nimonic 101 at ambient temperature

(a) Strain-controlled tests

		Values at mid-life							Frequency	Modulus $E_{1/4}$,	N_{25}	Location of failure			Remarks
		Strain range, %			Stress, MPa										
Partner ID	Specimen ID	$\Delta\varepsilon_t$	$\Delta\varepsilon_p$	$\Delta\varepsilon_e$	σ_{max}	σ_{min}	$\Delta\sigma$	σ_m	Hz	GPa	cycles	c, mm	c_0, mm	θ_c, degrees	
A	AVB31	1.002	0.166	0.836	852.66	-885.60	1738.26	-16.47	0.1	219.9	7853	NR	NR	NR	
A	AVB42	0.998	0.160	0.838	841.04	-886.16	1727.20	-22.56	0.1	216.3	9125	31.99	8.31	315	(2)
A	AVB43	1.012	0.171	0.841	872.58	-868.69	1741.27	1.94	0.1	220.8	8580	19.72	-3.96	250	
A	AVB45	0.999	0.158	0.841	812.91	-919.93	1732.84	-53.51	0.1	214.2	9112	30.47	6.79	10	(1)
B	AVB08	1.009	0.209	0.800	854.10	-891.30	1745.40	-18.60	0.1	226.1	7654	18.4	-1.59	160	
B	AVB09	1.008	0.177	0.832	859.70	-887.10	1746.80	-13.70	0.1	212.3	9631	26.9	6.91	270	(1)
B	AVB10	1.010	0.183	0.827	860.60	-887.50	1748.10	-13.45	0.1	226.2	7916	20.6	0.61	160	
C	AVB59	1.000	0.210	0.790	861.00	-848.00	1709.00	6.50	0.1	224.0	6440	27	7.01	20	(1)
C	AVB62	1.000	0.200	0.800	815.00	-876.00	1691.00	-30.50	0.1	221.0	6471	23	3.01	140	
C	AVB65	1.000	0.210	0.790	895.00	-826.00	1721.00	34.50	0.1	225.0	4701	28	8.01	180	(2)
D	AVB51	1.000	0.164	0.836	860.00	-888.00	1748.00	-14.00	0.1	222.5	10680	19	1.63	330	(3)
D	AVB52	1.000	0.160	0.840	857.00	-887.00	1744.00	-15.00	0.1	221.8	9780	22	4.63	210	
D	AVB53	1.000	0.160	0.840	853.00	-891.00	1744.00	-19.00	0.1	221.9	(4)	(4)	(4)	(4)	(4)
D	AVB57	1.000	0.160	0.840	850.00	-897.00	1747.00	-23.50	0.1	220.8	9643	26	8.63	250	(2)
E	AVB70	1.000	0.166	0.834	856.00	-858.00	1714.00	-1.00	0.1	217.1	6365	13	-5.77	315	(1)
E	AVB72	1.000	0.156	0.844	813.00	-886.00	1699.00	-36.50	0.1	212.9	7384	11.5	-7.27	270	(1)
E	AVB73	1.000	0.162	0.838	831.00	-873.00	1704.00	-21.00	0.1	214.1	7031	21.5	2.73	225	

NA Not applicable
NR Not reported
(1) Failure outside the gauge length
(2) Failure outside the parallel length
(3) Values taken at N = 3289
(4) Invalid test. Fracture at knife-groove (located in specimen's shoulders)

Table 9. (Continuation)

(b) Stress-controlled tests

Partner ID	Specimen ID	Values at mid-life: Strain range, % $\Delta\varepsilon_t$	$\Delta\varepsilon_p$	$\Delta\varepsilon_e$	Stress, MPa σ_{max}	σ_{min}	$\Delta\sigma$	σ_m	Frequency Hz	Modulus $E_{1/4}$, GPa	N_{25} cycles	Location of failure: c, mm	c_0, mm	θ_c, degrees	Remarks
A	AVB44	NA	NA	NA	600.0	-600.0	1200.0	0.0	1.0	NR	70533	20.36	-3.32	270	
A	AVB37	NA	NA	NA	600.0	-600.0	1200.0	0.0	1.0	NR	89123	24.55	0.87	315	
A	AVB38	NA	NA	NA	600.0	-600.0	1200.0	0.0	1.0	NR	84428	20.15	-3.53	170	
A	AVB40	NA	NA	NA	600.0	-600.0	1200.0	0.0	1.0	NR	109964	23.7	0.02	240	
B	AVB04	NA	NA	NA	600.9	-601.2	1202.1	-0.2	1.0	223.3	83326	28.8	8.81	135; 186	(2)
B	AVB05	NA	NA	NA	600.8	-601.2	1202.0	-0.2	1.0	222.9	82840	12.1	-7.89	90	(1)
B	AVB06	NA	NA	NA	600.8	-601.3	1202.1	-0.3	1.0	223.5	72142	11.6	-8.39	5	(2)
C	AVB61	NA	NA	NA	670.0	-650.0	1320.0	10.0	1.0	NR	(44638)	68	48.01	180	(4), (5)
C	AVB63	NA	NA	NA	680.0	-640.0	1320.0	20.0	1.0	NR	(49397)	27	7.01	170	(5)
C	AVB64	NA	NA	NA	645.0	-675.0	1320.0	-15.0	1.0	NR	(41176)	22	2.01	270	(5)
D	AVB54	NA	NA	NA	600.0	-600.0	1200.0	0.0	1.0	NR	92405	19	1.63	270	
D	AVB55	NA	NA	NA	600.0	-600.0	1200.0	0.0	1.0	NR	89698	17	-0.37	330	
D	AVB56	NA	NA	NA	600.0	-600.0	1200.0	0.0	1.0	NR	(49583)	(3)	(3)	(3)	(3)
E	AVB68	NA	NA	NA	599.9	-599.9	1199.8	0.0	1.0	214.1	81908	16	-2.77	215	
E	AVB69	NA	NA	NA	599.8	-600.0	1199.8	-0.1	1.0	219.5	96773	27	8.23	60	
E	AVB71	NA	NA	NA	601.3	-601.4	1202.7	-0.1	1.0	217.8	81846	12.5	-6.27	225	

NA Not applicable
NR Not reported
(1) Failure outside the gauge length
(2) Failure outside the parallel length
(3) Invalid test. Fracture at knife-groove (located in specimen's shoulders)
(4) Invalid test. Fracture at specimen's top button head
(5) Invalid test. Stress range is not in accordance with specifications

Table 10. Uncertainty budget spreadsheet for the determination of Young's modulus (In accordance with UNCERT CoP 02 [13])

Mathematical formulae used for calculations
Axial force where dP/P = ± 2.0%
Specimen diameter where 2.dd/d = ± 0.25%
Axial strain where dε/ε = ± 4.0%

SOURCE OF UNCERTAINTY	VALUE ± %	PROBABILITY DISTRIBUTION	DIVISOR	STANDARD UNCERTAINTY ± %
Axial force	1.5	Normal	1	1.5
Specimen diameter	0.25	Rectangular	√ 3	0.14
Axial strain	4.0	Rectangular	√ 3	2.31
Combined standard Uncertainty		Assumed normal		2.76
Expanded uncertainty (See note below)		Assumed normal (k_{95} = 2)		**5.5**

The expanded uncertainty calculated above is based on a standard uncertainty multiplied by a coverage factor k = 2, providing a level of confidence of approximately 95%. The uncertainty analysis was carried out in accordance with UNCERT CoP 02 [13].

Table 11. Uncertainty budget spreadsheet for strain-controlled tests at $\Delta\varepsilon_t$ = 1.0% in ambient conditions (In accordance with UNCERT CoP 02 [13])

Measurand N_{fmean} = 8997 cycles (= Mean value for partners A, B, D who had Class 5 alignment)
Total strain range, $\Delta\varepsilon_t$ = 1.0%
Material Nimonic 101
Test temperature 21 ± 2 °C

Mathematical formulae used for calculations

Bending where $dN_f/N_f = (\psi/\alpha)$ where α = -0.34 and ψ = 6%
Strain where $dN_f/N_f = (1/\alpha).\ \delta(\Delta\varepsilon_t)/\ \Delta\varepsilon_t$, α = -0.34 and $\delta(\Delta\varepsilon_t)/\ \Delta\varepsilon_t = \pm 0.75\%$

SOURCE OF UNCERTAINTY	VALUE %	PROBABILITY DISTRIBUTION	DIVISOR	STANDARD UNCERTAINTY ± %
Bending	-17.65	Rectangular	√ 3	10.19
Strain measurement	±2.21	Rectangular	√ 3	1.28
Combined standard Uncertainty		Assumed normal		10.27
Expanded uncertainty (See note below)		Assumed normal (k_{95} = 2)		**20.5**

The estimated number of cycles to failure, N_{25} = 8,997 cycles ± 20.5% (or ± 1,844 cycles)

The expanded uncertainty quoted is based on a standard uncertainty multiplied by a coverage factor k = 2, providing a level of confidence of approximately 95%. The uncertainty analysis was carried out in accordance with UNCERT CoP 02 [13].

Table 12. Uncertainty budget spreadsheet for stress-controlled tests at ambient temperature

Measurand N_{fmean} = 86051 (= Mean value for partners A, B, D who had Class 5 alignment)
Total strain range $\Delta\sigma$ = 1200 MPa
Material Nimonic 101
Test temperature 21 ± 2 °C

Mathematical formulae used for calculations

Bending where $dN_f/N_f = (\psi/\alpha)$ where α = -0.11 and ψ = 2%
Load cell where dP/P = ± 2.0%
Specimen diameter where 2.dd/d = ± 0.25%

SOURCE OF UNCERTAINTY	VALUE ± %	PROBABILITY DISTRIBUTION	DIVISOR	STANDARD UNCERTAINTY ± %
Specimen bending	-18.18	Rectangular	$\sqrt{3}$	10.50
Axial force	±1.5	Normal	1	1.5
Specimen diameter	±0.25	Rectangular	$\sqrt{3}$	0.14
Combined standard Uncertainty		Assumed normal		10.61
Expanded uncertainty (See note below)		Assumed normal (k_{95} = 2)		**21.2**

The estimated number of cycles to failure, N_{25} = 86051 cycles ± 21.2% (or ±18,243 cycles)

The expanded uncertainty quoted is based on a standard uncertainty multiplied by a coverage factor k = 2, providing a level of confidence of approximately 95%.

Table 13. Summary of strain-controlled LCF test data with superimposed bending (IFW data [14])

Test Series	β_{max}	Specimen	Test	$E_{1/4}$	f, Hz	Values at mid-life					N_{25}	N_{max} (1)	Location of Failure			Remarks
	%	ID	ID	GPa		$\Delta\varepsilon_t$, % (measured)	$\Delta\varepsilon_p$, % (measured)	σ_{max}, MPa	σ_{min}, MPa	$\Delta\sigma$, MPa	cycles	cycles	c, mm	c_o, mm	θ_c	
1	< 2	AVB82	D17	164.1	0.1002	0.502	0.019	423.2	-339.7	762.9	8349	8357	20.0	5.7	0°	
1	< 2	AVB86	D21	162.9	0.0973	0.514	0.022	457.8	-338.1	795.9	8842	8957	3.6	-10.8	100°	(3)
1	< 2	AVB92	D27	161.6	0.0996	0.496	0.023	430.2	-349.9	780.1	7390	7399	25.0	10.7	160°	(3)
4	< 2	AVB84	D19	167.9	0.0440	1.137	0.417	523.8	-549.6	1073.4	402	402	14.2	-0.2	225°	
4	< 2	AVB90	D25	162.3	0.0448	1.116	0.461	490.3	-512.6	1002.9	n.a.	301	17.9	3.6	340°	
4	< 2	AVB91	D26	160.9	0.0452	1.106	0.416	531.1	-559.1	1090.1	299	300	19.7	5.4	105°	
2	18 - 22	AVB78	D13	160.7	0.0998	0.501	0.018	444.0	-340.1	784.0	6764	6764	22.6	8.3	50°	(2)
2	18 - 22	AVB83	D18	161.5	0.0984	0.508	0.019	454.1	-328.8	782.9	n.a.	6633	11.3	-3.1	0°	
2	18 - 22	AVB87	D22	162.9	0.0977	0.513	0.023	446.2	-352.4	798.6	n.a.	6332	23.1	8.8	320°	(2)
5	18 - 22	AVB77	D12	161.5	0.0441	1.135	0.385	529.0	-541.1	1070.1	237	240	7.7	-6.7	0°	
5	18 - 22	AVB80	D15	159.9	0.0447	1.118	0.385	535.0	-547.8	1082.9	267	270	18.8	4.5	160°	
5	18 - 22	AVB85	D20	162.1	0.0442	1.131	0.402	528.5	-535.1	1063.6	260	263	20.7	6.4	180°	
3	38 - 42	AVB89	D24	160.0	0.0986	0.507	0.017	440.0	-342.0	781.0	7488	7681	3.4	-11.0	30°	(3)
3	38 - 42	AVB93	D28 (4)	159.0	0.0984	0.508	0.019	444.0	-330.0	774.0	8489	n.a.	23.3	9.0	180°	(2)
3	38 - 42	AVB94	D29 (5)	158.0	0.0983	0.508	0.015	429.0	-348.0	777.0	8453	8505	3.8	-10.6	225°	(3)
6	38 - 42	AVB75	D10	160.0	0.0451	1.108	0.409	524.8	-545.1	1069.9	190	192	19.8	5.5	270°	
6	38 - 42	AVB79	D14	158.0	0.0442	1.131	0.384	511.9	-506.9	1018.8	140	141	20.6	6.3	180°	
6	38 - 42	AVB81	D16	164.1	0.0442	1.130	0.379	524.5	-520.1	1044.5	165	166	4.7	-9.7	340°	(2)

(1) Number of cycles at termination of test.
(2) Failure outside the extensometer's gauge length of 15 mm.
(3) Failure outside the specimen's parallel length of 19.6 mm.
(4) Test interrupted at N=4320
(5) Test interrupted at N=6000

Table 14. Test equipment used in the mini VAMAS inter-laboratory LCF exercise at 850°C

Organisation		NPL	IFW	NRIM
Test machine model		Instron 8562	Schenck	MTS
Machine type		Servo-electric (2 column)	Servo-hydraulic (2 column)	Servo-hydraulic (2 column)
Frame capacity (+/- kN)		250	160	NR
Load cell capacity (+/- kN)		100	100	100
Class of machine		1	1	NR
Alignment method		Instron alignment fixture	Schenck alignment fixture	MTS alignment fixture
Alignment Class		5	5	5
Extensometer type		MTS 632-41F-11	Sandner EX H15 - 0.75 A	MTS 632.53E-4
Extensometer details	GL, mm	12.0	15.0	20.0
	Range, ± mm	2.4	0.75	NR
	Class	0.5	1	NR
Heating method		Furnace, 3 zones, split	Infrared	Induction
Thermocouple type		R	S	NR
Temperature variation along the specimen's parallel length, ±°C		848.6 - 851.4	847.5 - 851.5	840 to 850
Number of thermocouples		2	3	2
Thermocouple location		Parallel length	Parallel length	Specimen shoulder
Method of attachment		Wire, no insulation	Wire, insulated	Spot welded
Specimen type		Button head	Straight, long (Special design)	Straight shank (Similar to the NPL Type 1 shown in Fig. 24)
Specimen Dimensions, mm	d	8.00 ± 0.02	8.00 ± 0.01	8.00 ± 0.01
	l_p	16.0	19.6	20.0
	R	30.0	18.0	30.0
	L	120.0	556	150.0
Surface finish, R_a, ≤		0.07	0.23	NR

NR Not reported

Table 15. Summary of strain-controlled LCF tests on Nimonic 101 at 850°C (IFW data)

Test Series	β_{max}	Specimen	Test	$E_{1/4}$	f, Hz	Values at mid-life					N_{25}	N_{max} (1)	Location of Failure			Remarks
	%	ID	ID	GPa		$\Delta\varepsilon_t$, % (measured)	$\Delta\varepsilon_p$, % (measured)	σ_{max}, MPa	σ_{min}, MPa	$\Delta\sigma$, MPa	cycles	cycles	c, mm	c_o, mm	θ_c	
1	< 2	AVB82	D17	164.1	0.1002	0.502	0.019	423.2	-339.7	762.9	8349	8357	20.0	5.7	0°	
1	< 2	AVB86	D21	162.9	0.0973	0.514	0.022	457.8	-338.1	795.9	8842	8957	3.6	-10.8	100°	(2)
1	< 2	AVB92	D27	161.6	0.0996	0.496	0.023	430.2	-349.9	780.1	7390	7399	25.0	10.7	160°	(2)
4	< 2	AVB84	D19	167.9	0.0440	1.137	0.417	523.8	-549.6	1073.4	402	402	14.2	-0.2	225°	
4	< 2	AVB90	D25	162.3	0.0448	1.116	0.461	490.3	-512.6	1002.9	n.a.	301	17.9	3.6	340°	
4	< 2	AVB91	D26	160.9	0.0452	1.106	0.416	531.1	-559.1	1090.1	299	300	19.7	5.4	105°	

(1) Number of cycles at termination of test.
(2) Failure outside the specimen's parallel length of 19.6 mm.

Table 16. Summary of strain-controlled LCF tests on Nimonic 101 at 850°C (NRIM data)

Specimen ID	Test ID	Values at mid-life: Strain range, % $\Delta\varepsilon_t$	$\Delta\varepsilon_p$	$\Delta\varepsilon_e$	Stress, MPa: Tensile amplitude	Compressive amplitude	Range	Mean	Modulus E_0, GPa	Modulus $E_{1/4}$, GPa	N_x (x = 25%)	Location of failure: c_0, mm	θ_c, degrees	Remarks
293EAK	293EAK	1.200	0.5400	0.660	457.00	484.00	941.00	-13.50	NA	154.0	169	NA	NA	
321EAK	321EAK	1.200	0.5500	0.650	462.00	490.00	952.00	-14.00	NA	157.0	146	NA	NA	
309EAK	309EAK	1.200	0.5400	0.660	460.00	492.00	952.00	-16.00	NA	155.0	169	NA	0	
295EAK	295EAK	1.200	0.5000	0.700	496.00	531.00	1027.00	-17.50	NA	157.0	162	NA	90	
260EAK	260EAK	1.200	0.5520	0.648	442.00	471.00	913.00	-14.50	NA	157.0	177	NA	NA	
281EAK	281EAK	1.200	0.5560	0.644	446.00	472.00	918.00	-13.00	NA	156.0	181	NA	270	
314EAK	314EAK	0.500	0.0400	0.460	376.00	359.00	735.00	8.50	NA	155.0	5264	NA	NA	
274EAK	274EAK	0.500	0.0190	0.481	400.00	377.00	777.00	11.50	NA	160.0	8708	NA	315	
262EAK	262EAK	0.500	0.0340	0.466	384.00	356.00	740.00	14.00	NA	156.0	4930	NA	270	
297EAK	297EAK	0.500	0.0270	0.473	401.00	362.00	763.00	19.50	NA	160.0	7942	NA	315	

NA = Not available

Table 17. Uncertainty budget spreadsheet for strain-controlled tests at $\Delta\varepsilon_t$ = 1.2% and 850°C (In accordance with UNCERT CoP 02 [13])

Measurand	N_{fmean} = 320 cycles (For NPL only. Average of 4 tests)
Total strain range	$\Delta\varepsilon_t$ = 1.2%
Material	Nimonic 101
Test temperature	850 ± 4 °C

Mathematical formulae used for calculations

Bending	where $dN_f/N_f = (\psi/\alpha)$ where α = -0.32 and ψ = 10%
Strain	where $dN_f/N_f = (1/\alpha).\ \delta(\Delta\varepsilon_t)/\ \Delta\varepsilon_t$, α = -0.32 and $\delta(\Delta\varepsilon_t)/\ \Delta\varepsilon_t = \pm 0.75\%$
Temperature	$dN_f/N_f = c_T.\ \delta T/T$, where c_T = -3.44 cycles/°C and $\delta T/T = \pm$ 4 °C

SOURCE OF UNCERTAINTY	VALUE %	PROBABILITY DISTRIBUTION	DIVISOR	STANDARD UNCERTAINTY ± %
Bending	-31.3	Rectangular	√ 3	18.1
Strain measurement	±2.3	Rectangular	√ 3	1.3
Temperature	±4.3	Rectangular	√ 3	2.5
Combined standard Uncertainty		Assumed normal		18.3
Expanded uncertainty (See note below)		Assumed normal (k_{95} = 2)		**37**

The estimated number of cycles to failure, N_{25} = 320 cycles ± 37% (or ± 118 cycles)

The expanded uncertainty quoted is based on a standard uncertainty multiplied by a coverage factor k = 2, providing a level of confidence of approximately 95%. The uncertainty analysis was carried out in accordance with UNCERT CoP 02 [13].

Table 18. Uncertainty budget spreadsheet for strain-controlled tests at $\Delta\varepsilon_t$ = 0.5% and 850°C (In accordance with UNCERT CoP 02 [13])

Measurand	N_{fmean} = 18345 cycles (For NPL only. Average of 3 tests)
Total strain range	$\Delta\varepsilon_t$ = 0.50%
Material	Nimonic 101
Test temperature	850 ± 4 °C

Mathematical formulae used for calculations

Bending	where $dN_f/N_f = (\psi/\alpha)$ where α = -0.12 and ψ = 1%
Strain	where $dN_f/N_f = (1/\alpha).\ \delta(\Delta\varepsilon_t)/\ \Delta\varepsilon_t$, α = -0.12 and $\delta(\Delta\varepsilon_t)/\ \Delta\varepsilon_t = \pm 0.75\%$
Temperature	$dN_f/N_f = c_T.\ \delta T/T$, where c_T = -473 cycles/°C and $\delta T/T = \pm 4$ °C

SOURCE OF UNCERTAINTY	VALUE %	PROBABILITY DISTRIBUTION	DIVISOR	STANDARD UNCERTAINTY ± %
Bending	-8.3	Rectangular	√ 3	4.8
Strain measurement	±6.5	Rectangular	√ 3	3.8
Temperature	±10.3	Rectangular	√ 3	6.0
Combined standard Uncertainty		Assumed normal		8.6
Expanded uncertainty (See note below)		Assumed normal (k_{95} = 2)		**17**

The estimated number of cycles to failure, N_{25} = 18345 cycles ± 17% (or ± 3119 cycles)

The expanded uncertainty quoted is based on a standard uncertainty multiplied by a coverage factor k = 2, providing a level of confidence of approximately 95%. The uncertainty analysis was carried out in accordance with UNCERT CoP 02 [13].

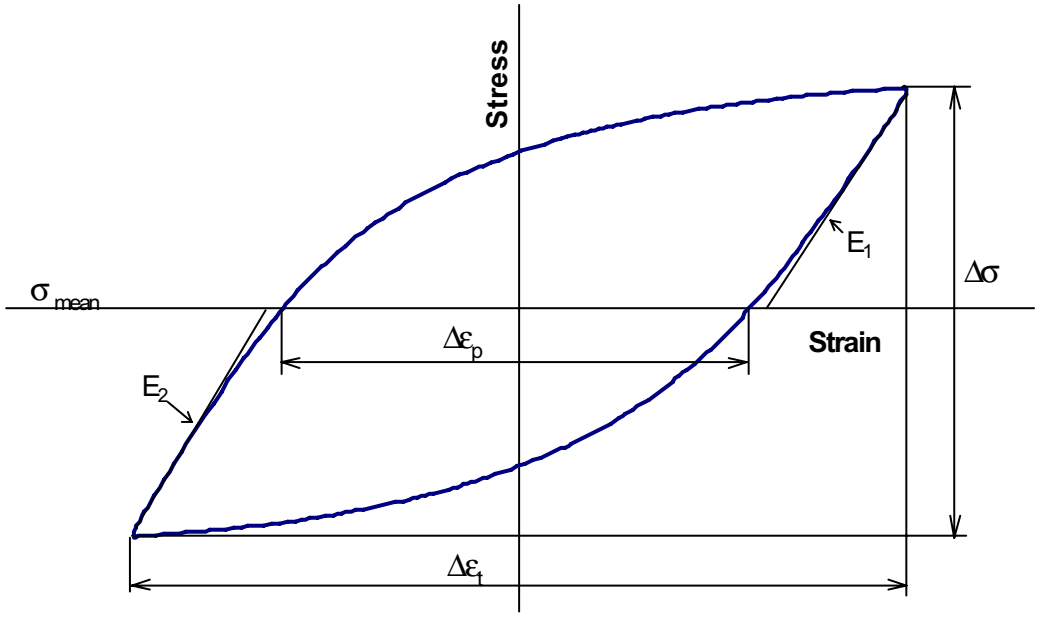

a. Parameters used in strain-controlled fatigue testing

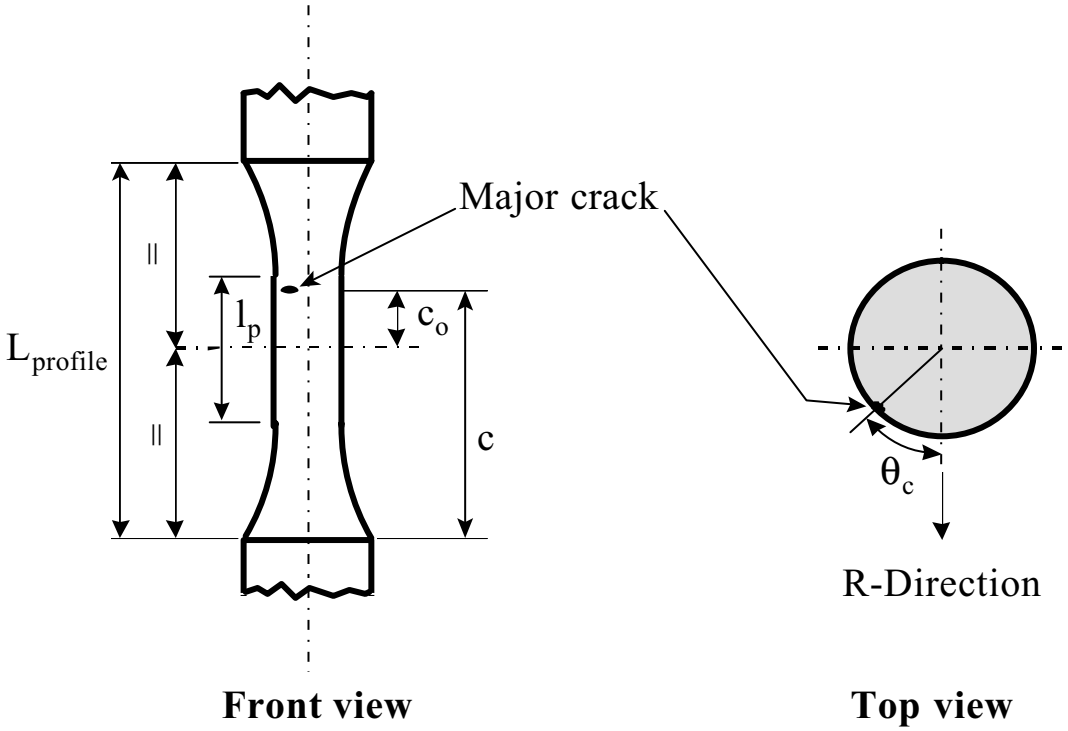

b. Parameters used to describe the location of the major crack initiation site.

Figure 1. Illustrations of the definitions used in LCF testing

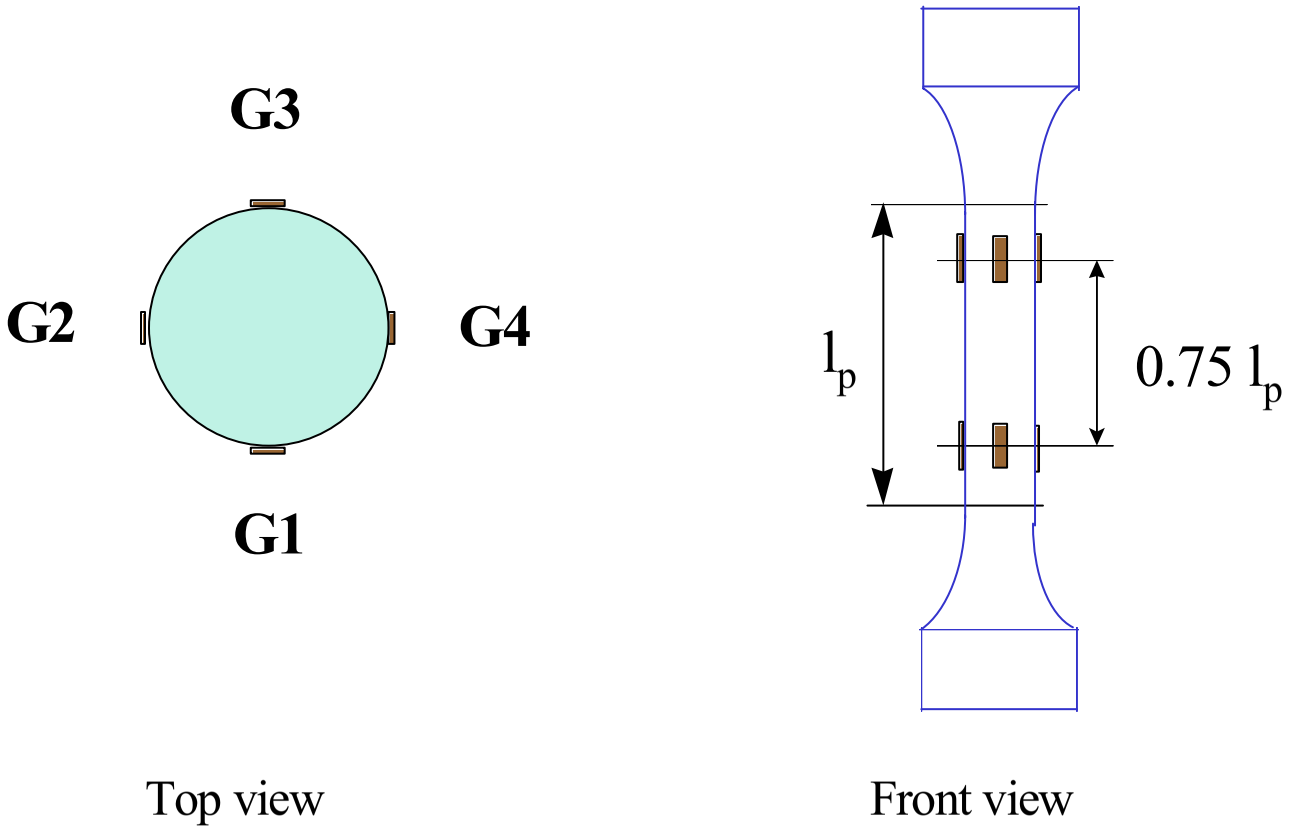

Figure 2. Schematic diagram showing the locations of strain gauges for machine alignment and specimen bending measurements

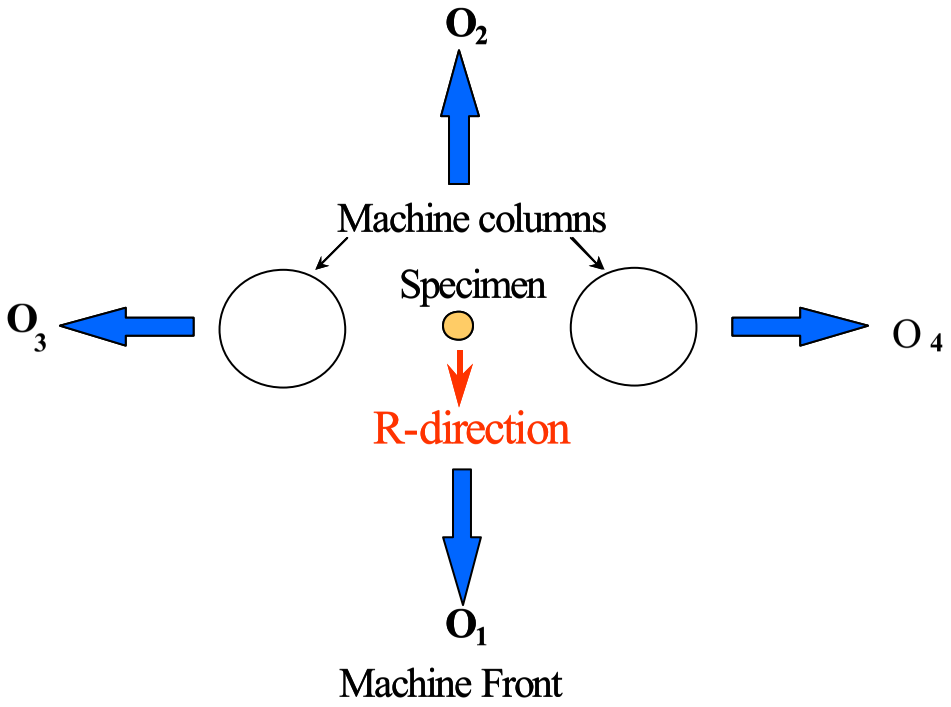

Figure 3. Definitions of the R-direction and specimen orientations used in alignment and specimen bending measurements

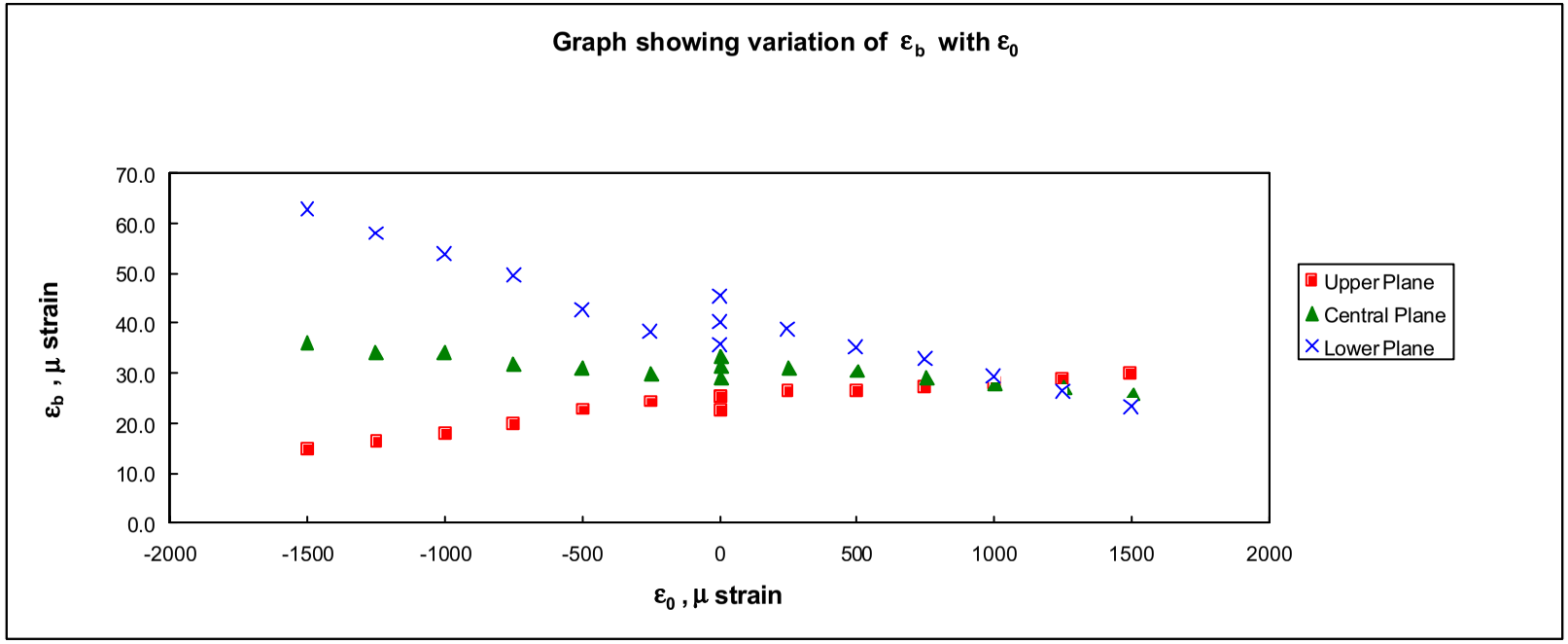

Figure 4. An example of the variation of the maximum bending strain with the applied average axial strain

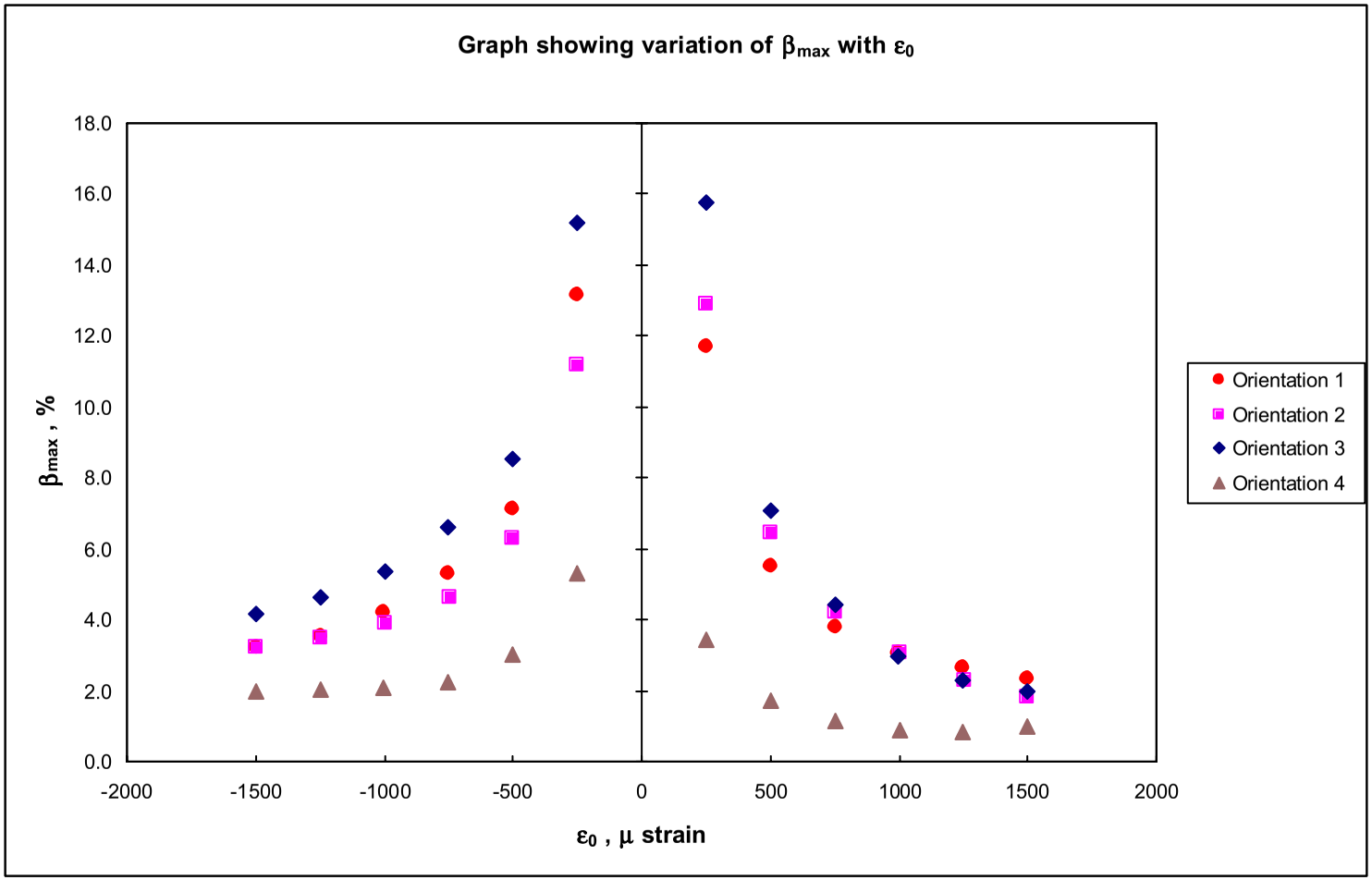

Figure 5. An example of the variation of the maximum percent bending with both specimen orientation and the applied average axial strain

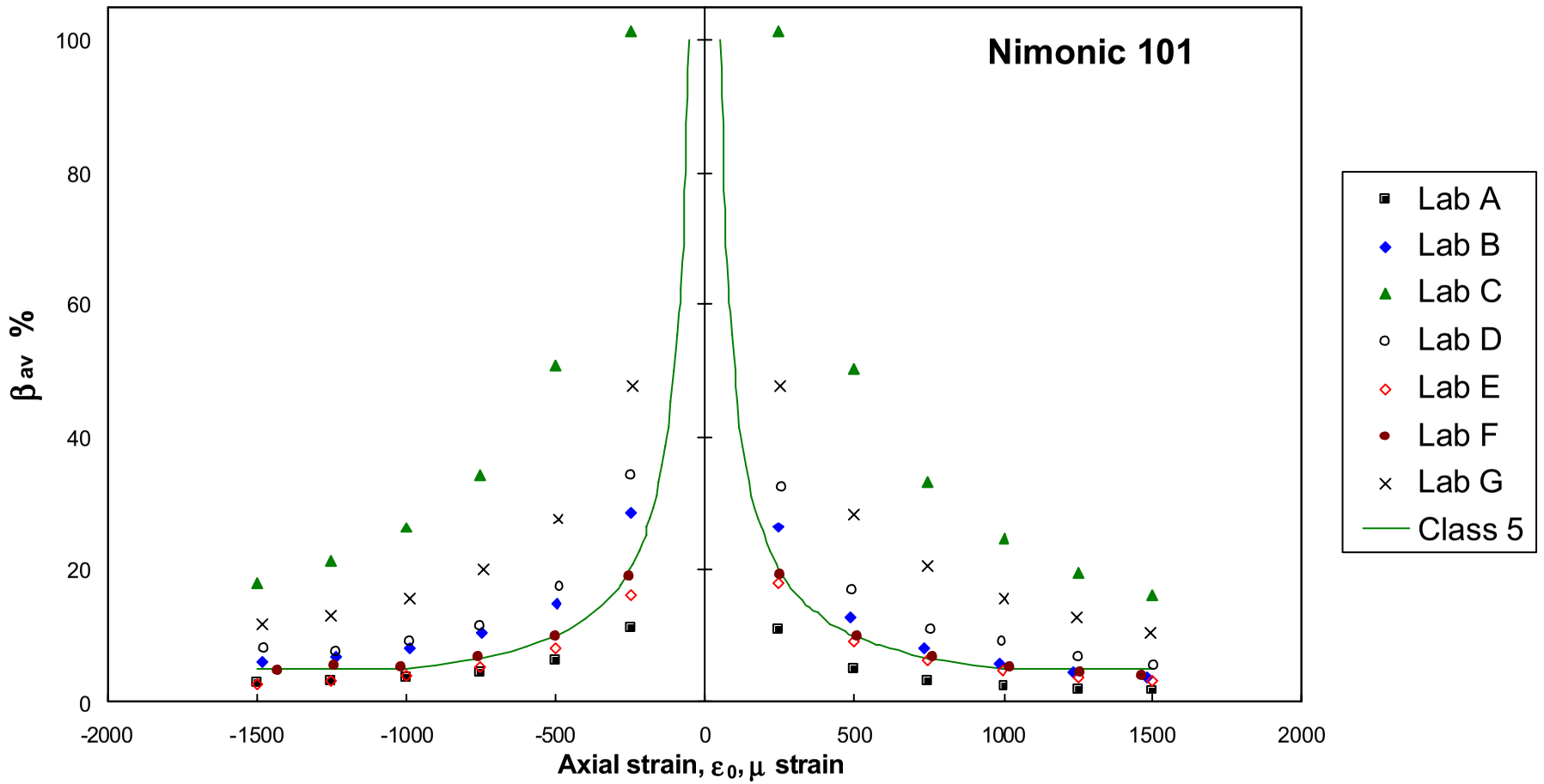

Figure 6. Inter-laboratory results of the maximum percent bending using Nimonic 101 test specimens

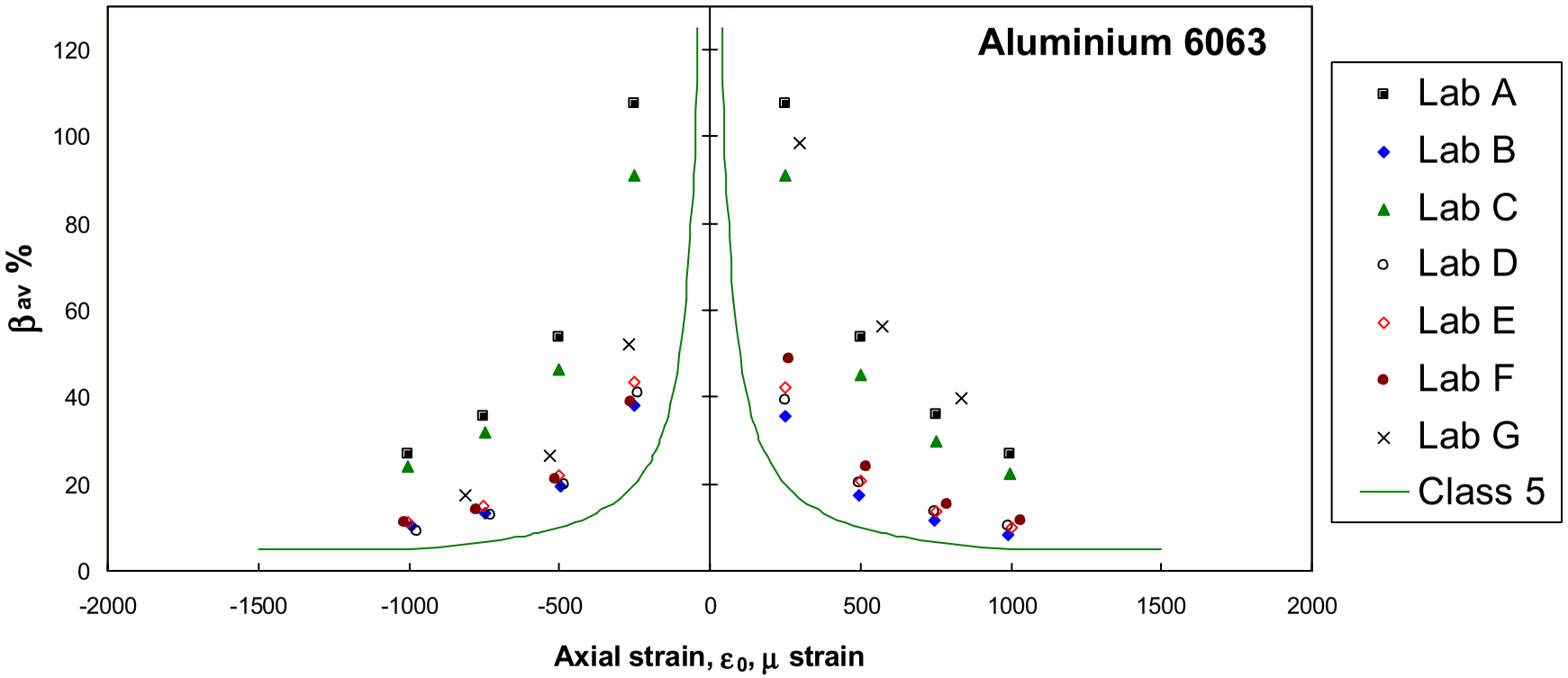

Figure 7. Inter-laboratory results of the maximum percent bending using aluminium alloy 6063 test specimens

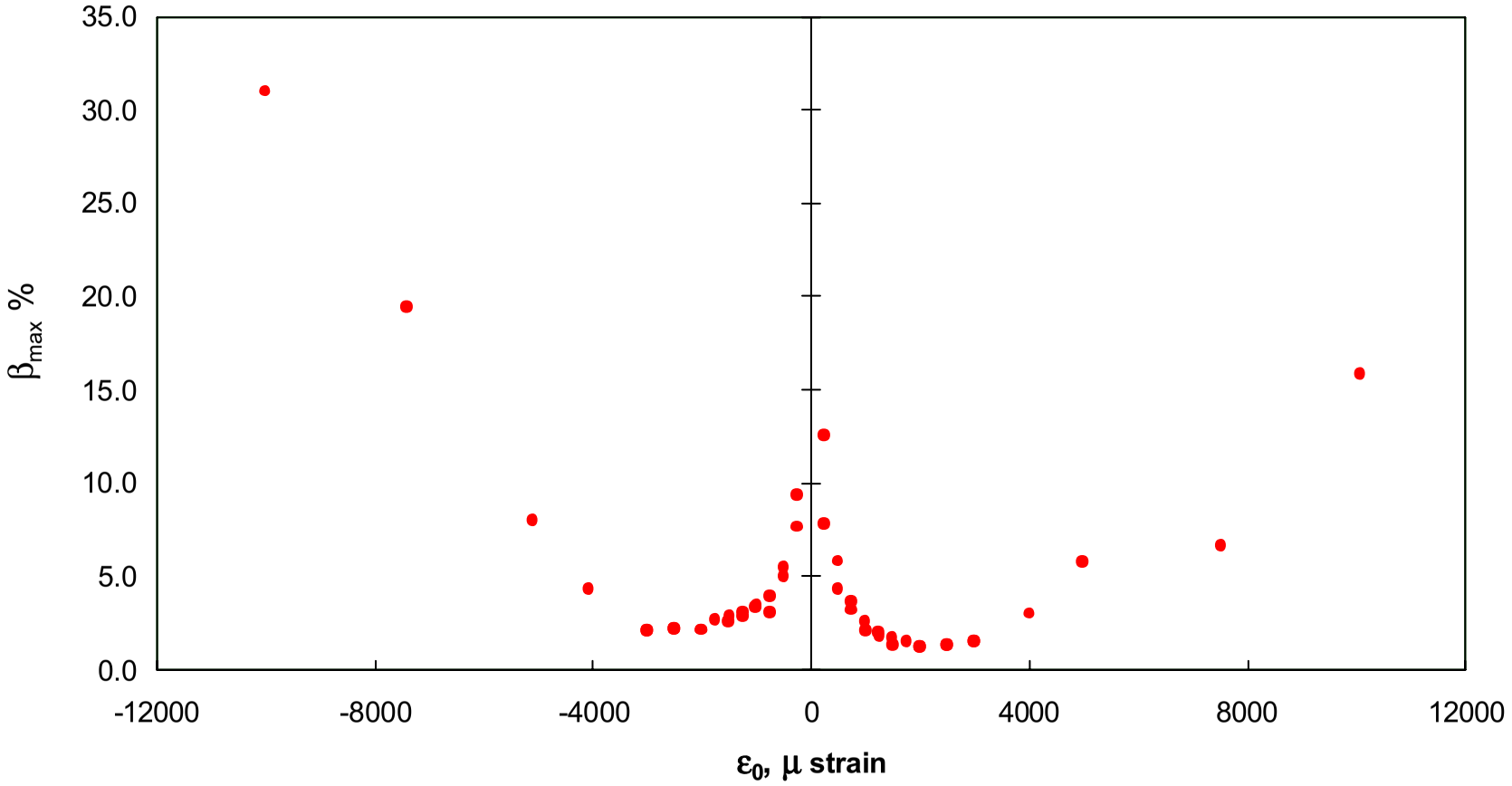

Figure 8. An example of the variation of the maximum percent bending during plastic deformation in a Nimonic 101 test specimen

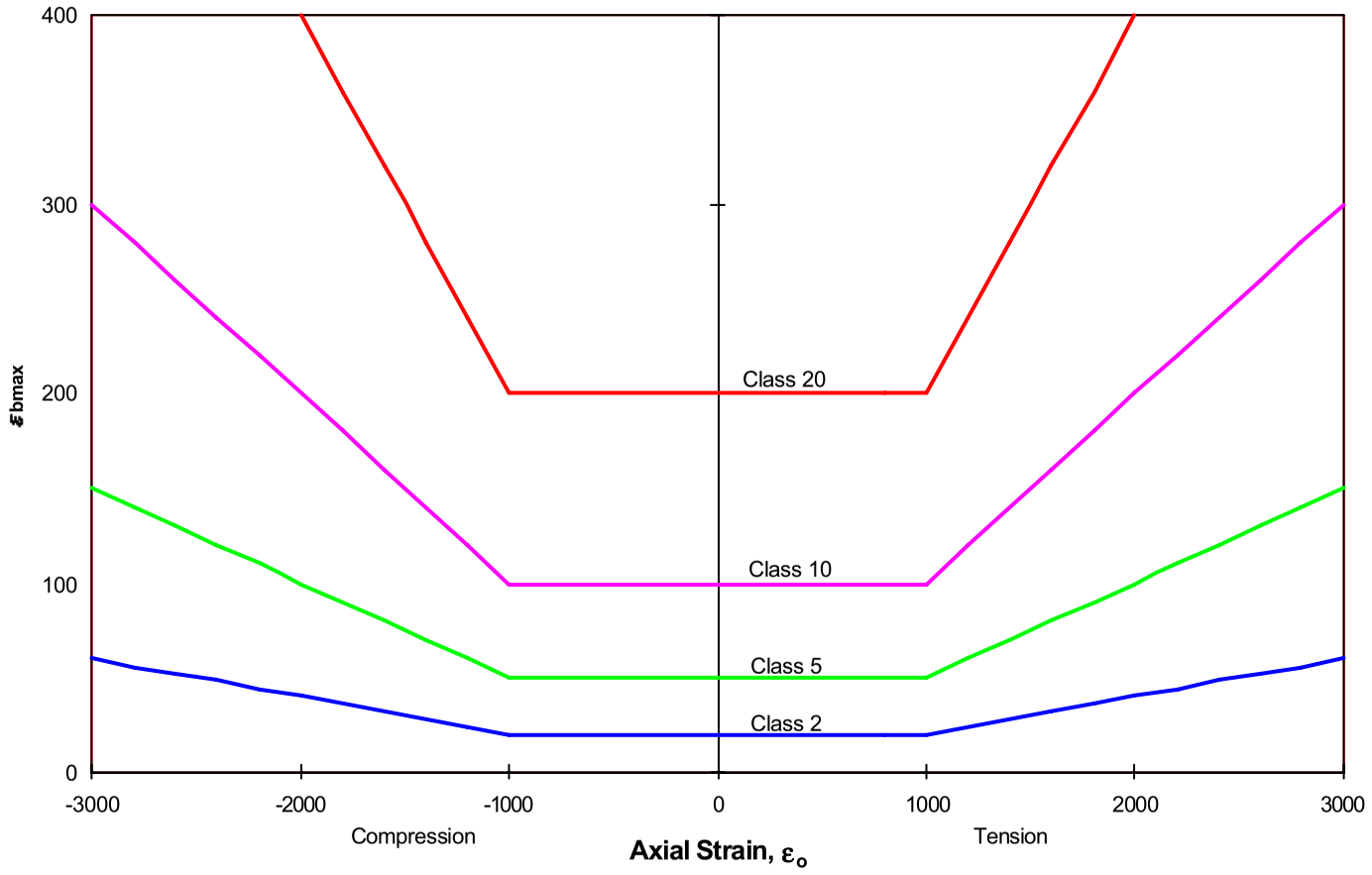

Figure 9. Machine alignment classification system [11]

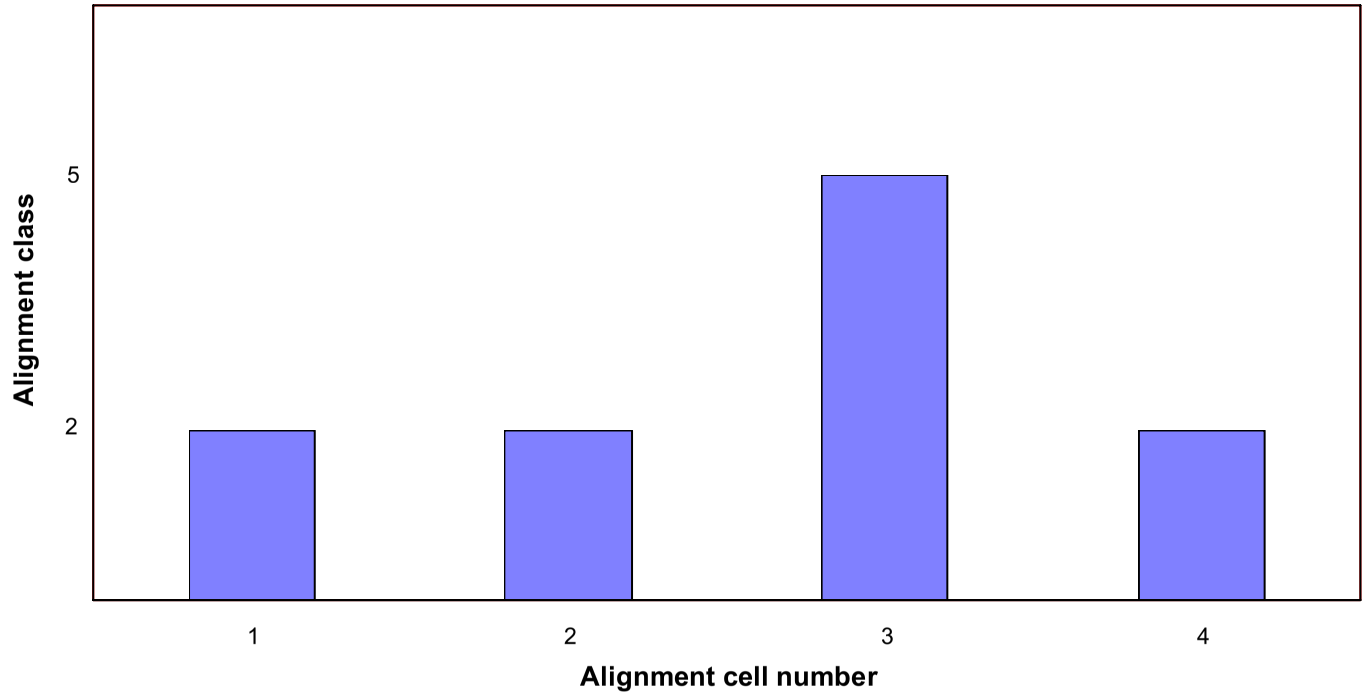

Figure 10. An example of the reproducibility of alignment measurement for a well-aligned test machine

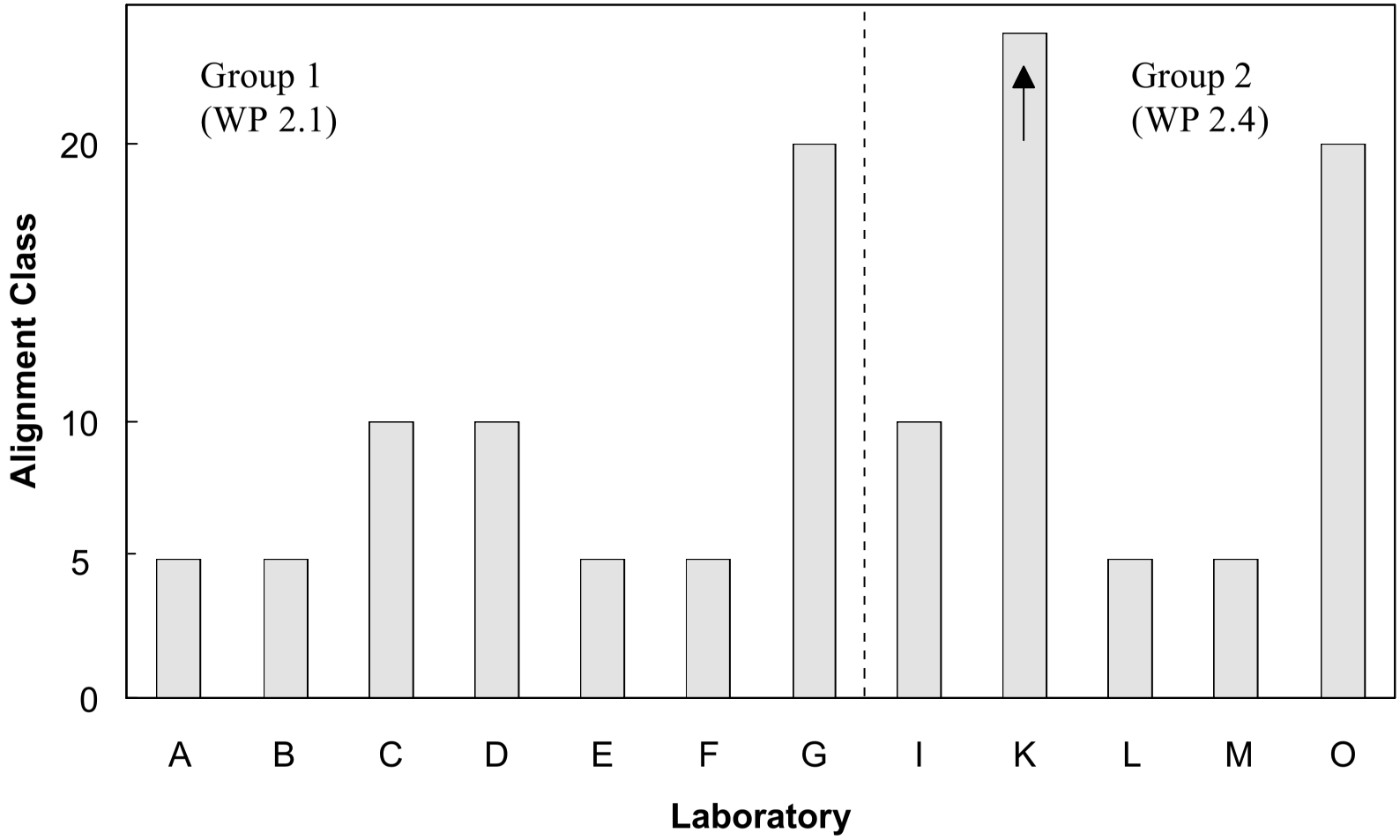

Figure 11. Inter-comparison of the machine alignment class

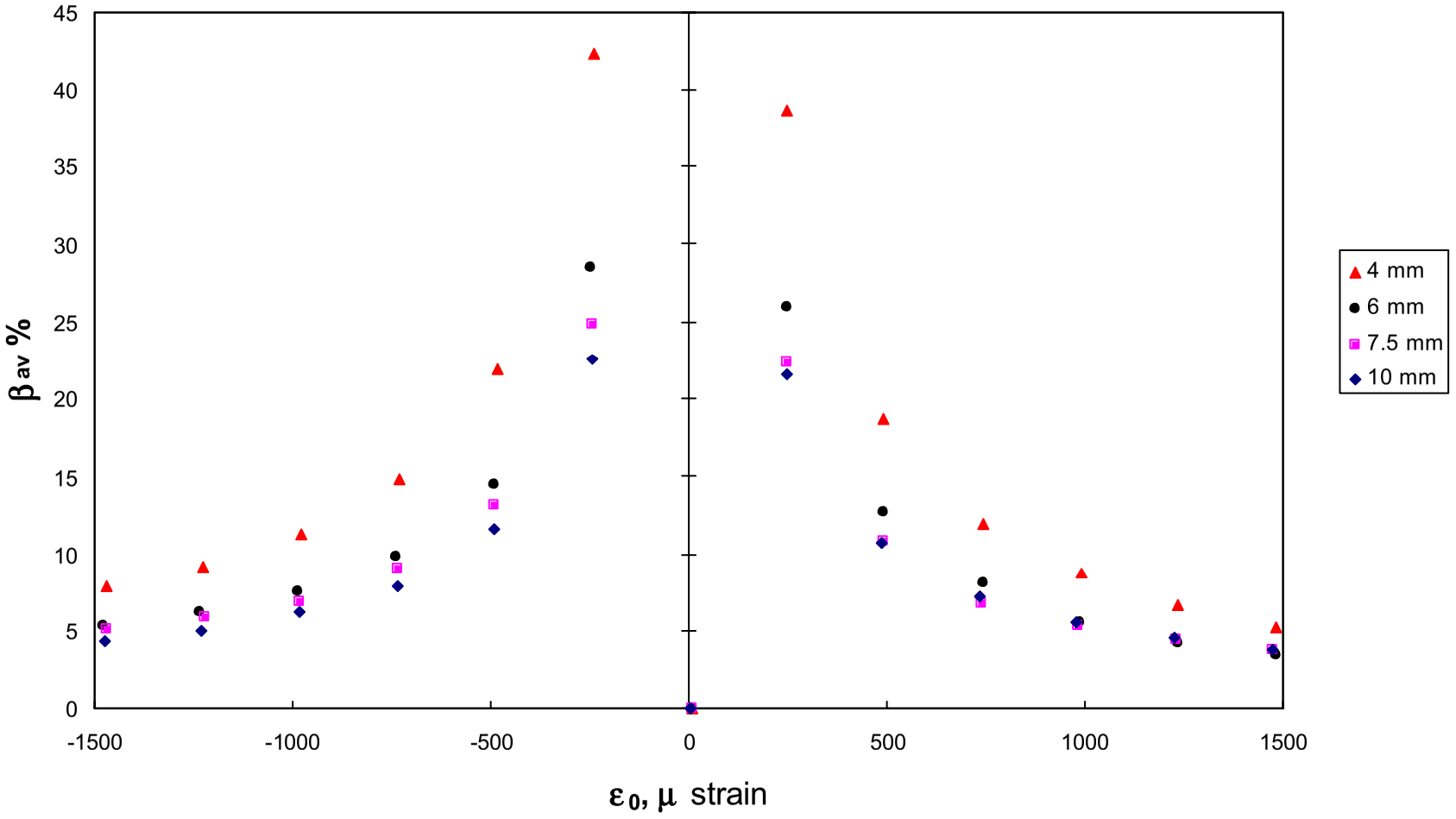

Figure 12. Variation of percent bending, β_{av}, with specimen diameter

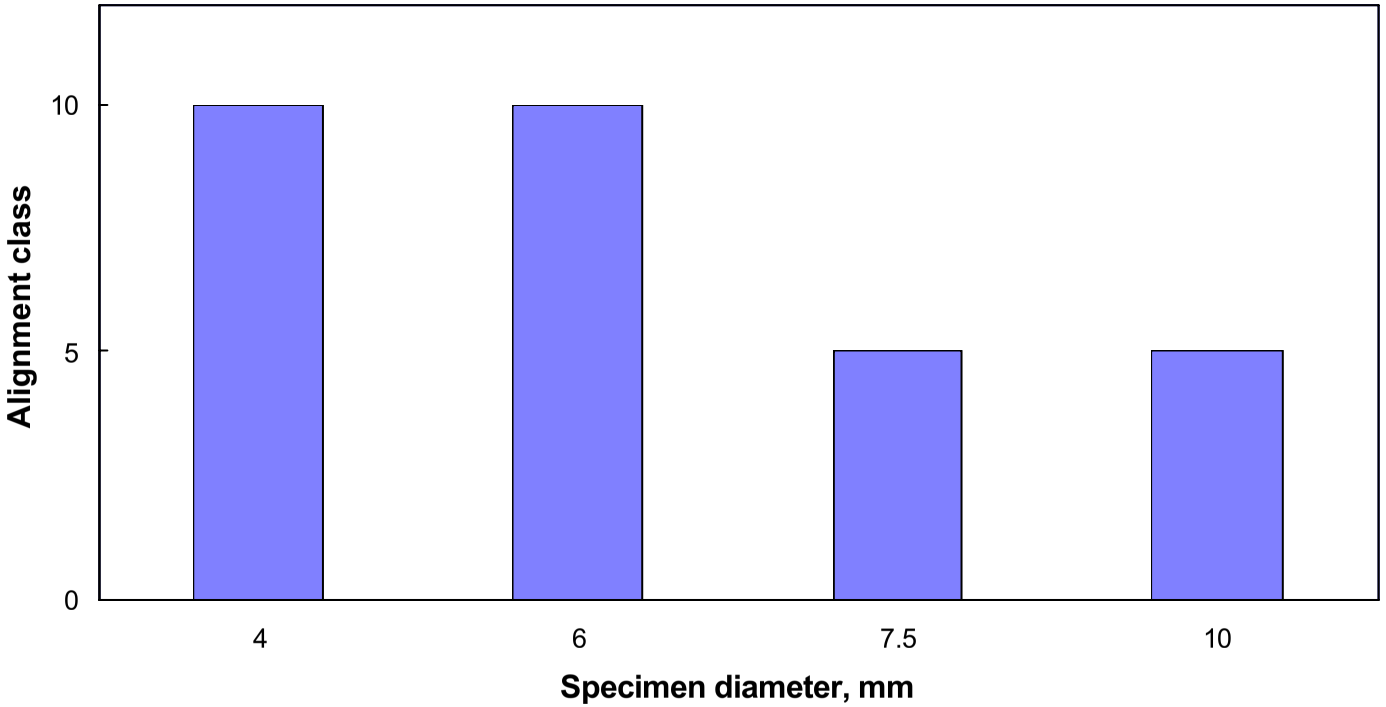

Figure 13. Machine alignment class according to alignment cells with different diameters

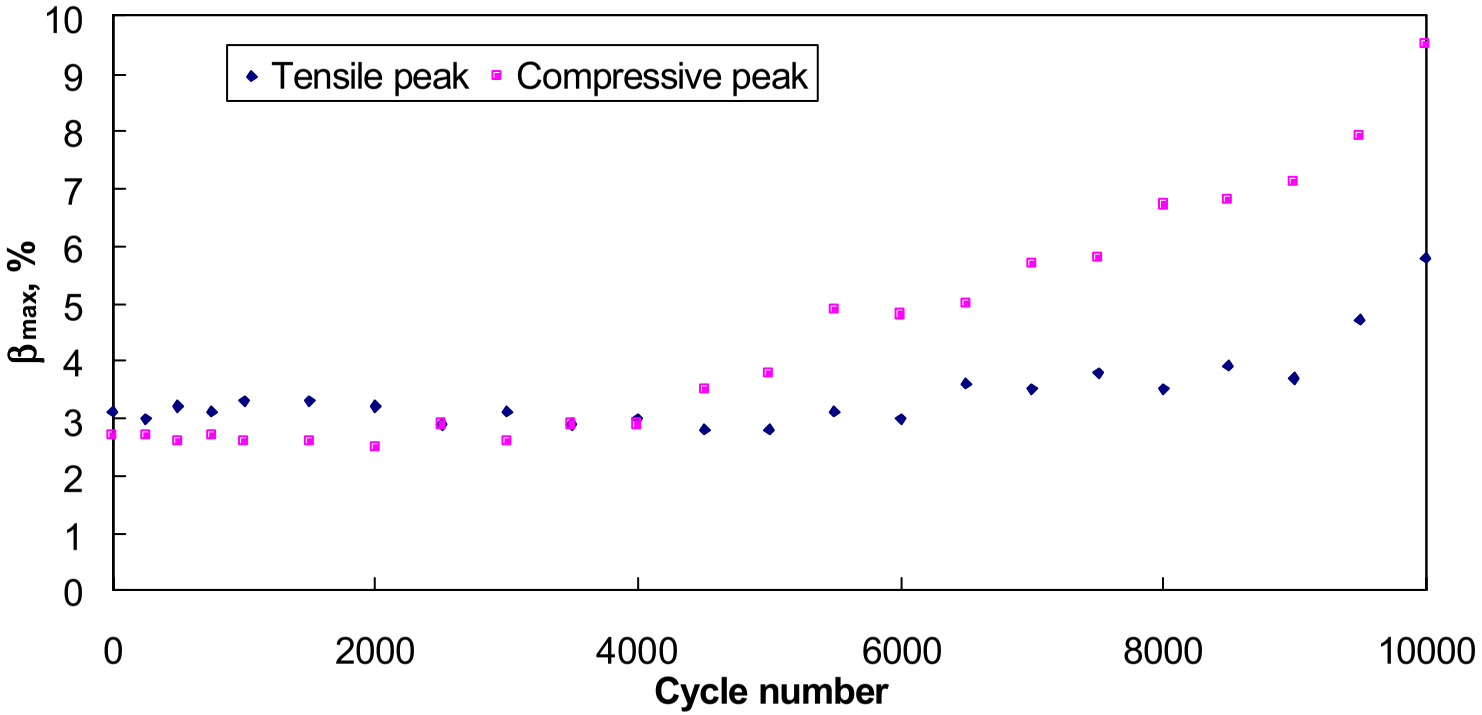

Figure 14. Graph showing an increase of percent bending during a fatigue test

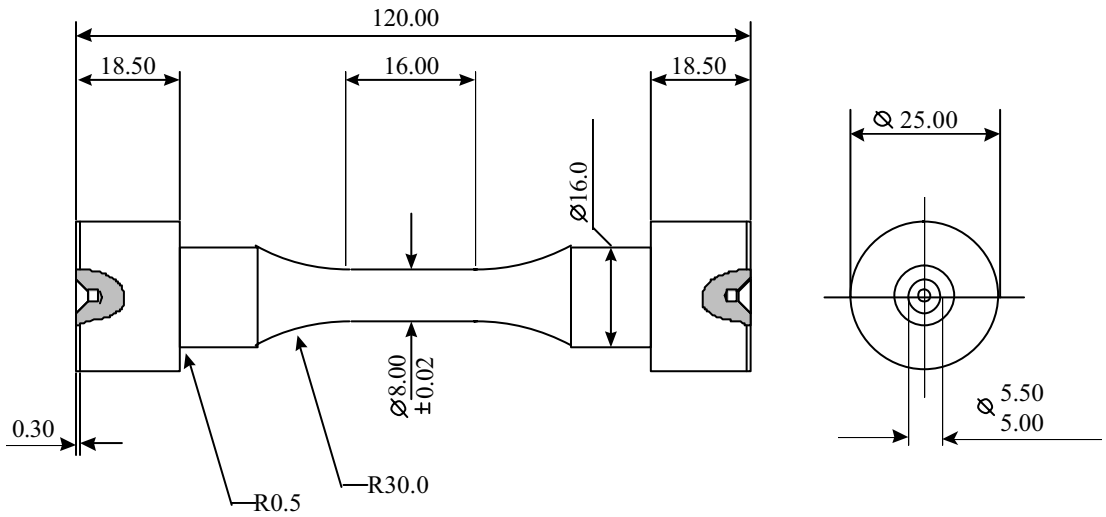

Figure 15. NPL specimen used for the LCF tests at ambient and elevated temperatures

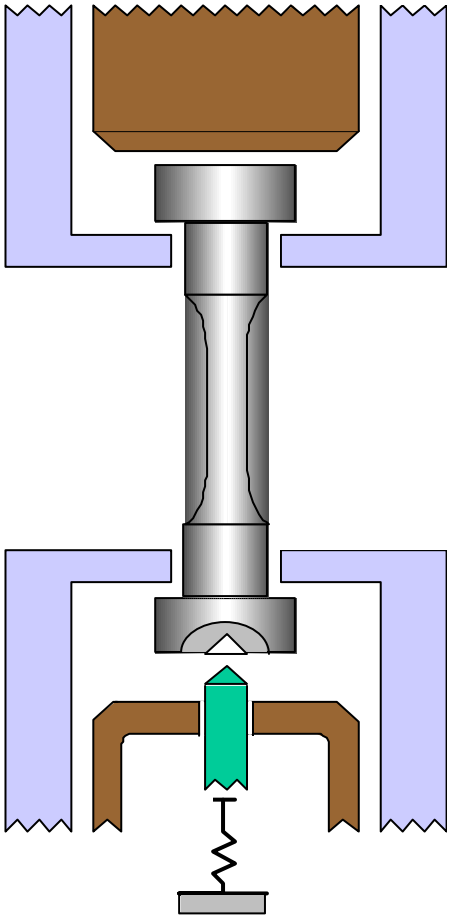

Figure 16. Schematic diagram of the new specimen grip system utilised at NPL for this work

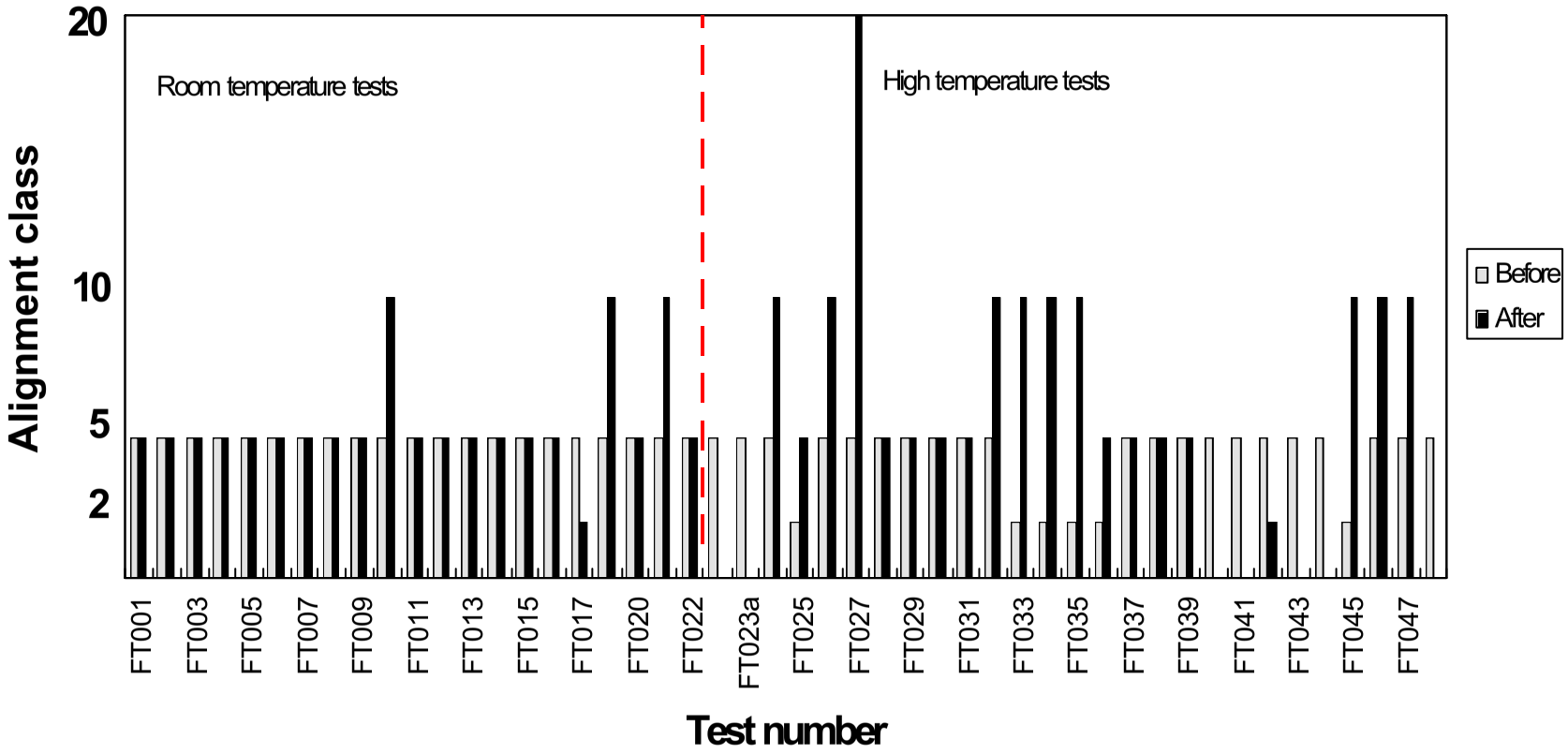

Figure 17. Machine alignment before and after LCF tests (NPL tests)

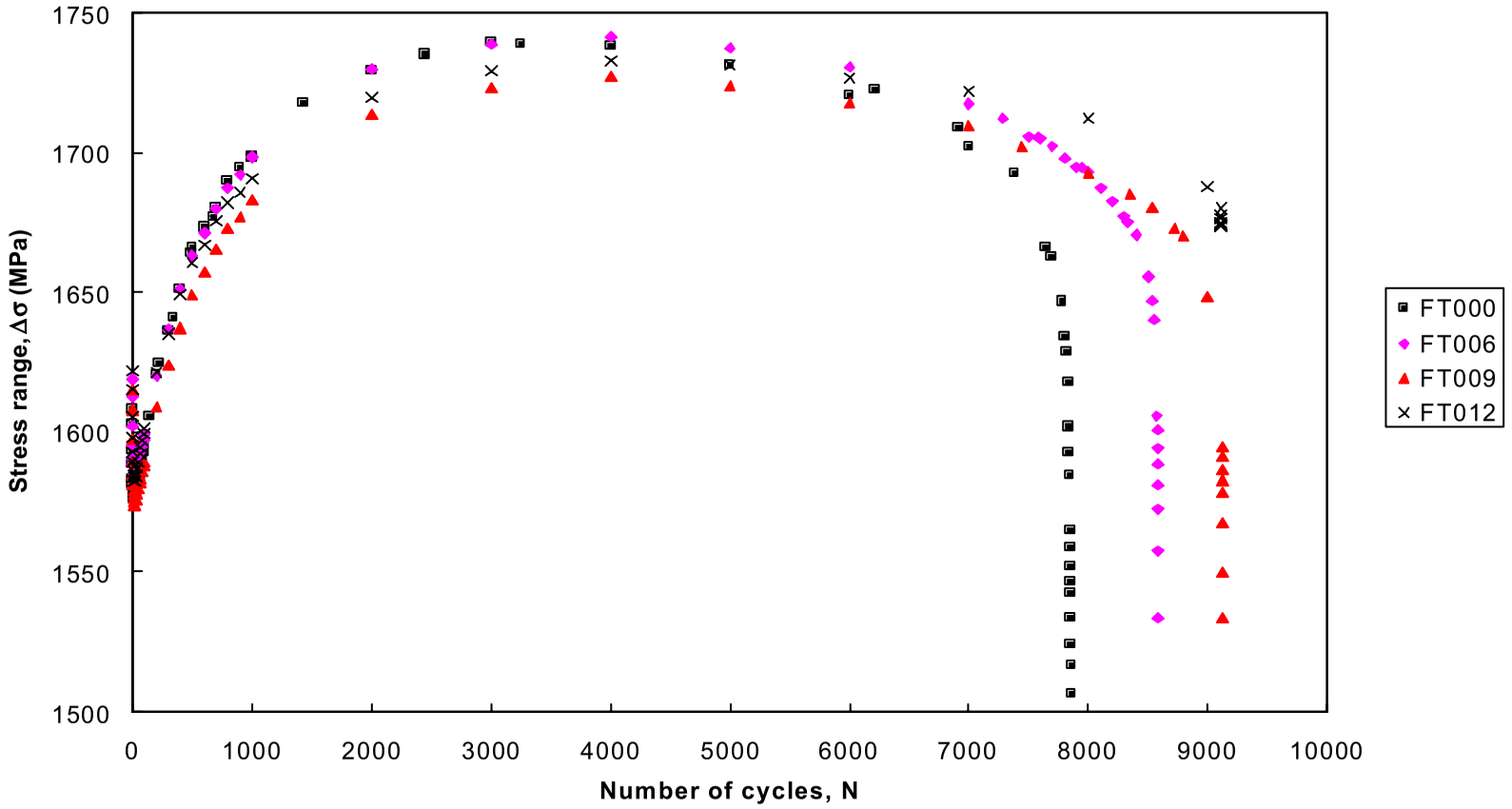

Figure 18. Variation of the stress range during strain-controlled fatigue tests on Nimonic 101 at ambient temperature (Baseline data; repeat tests at $\Delta\varepsilon_t$ = 1.0%)

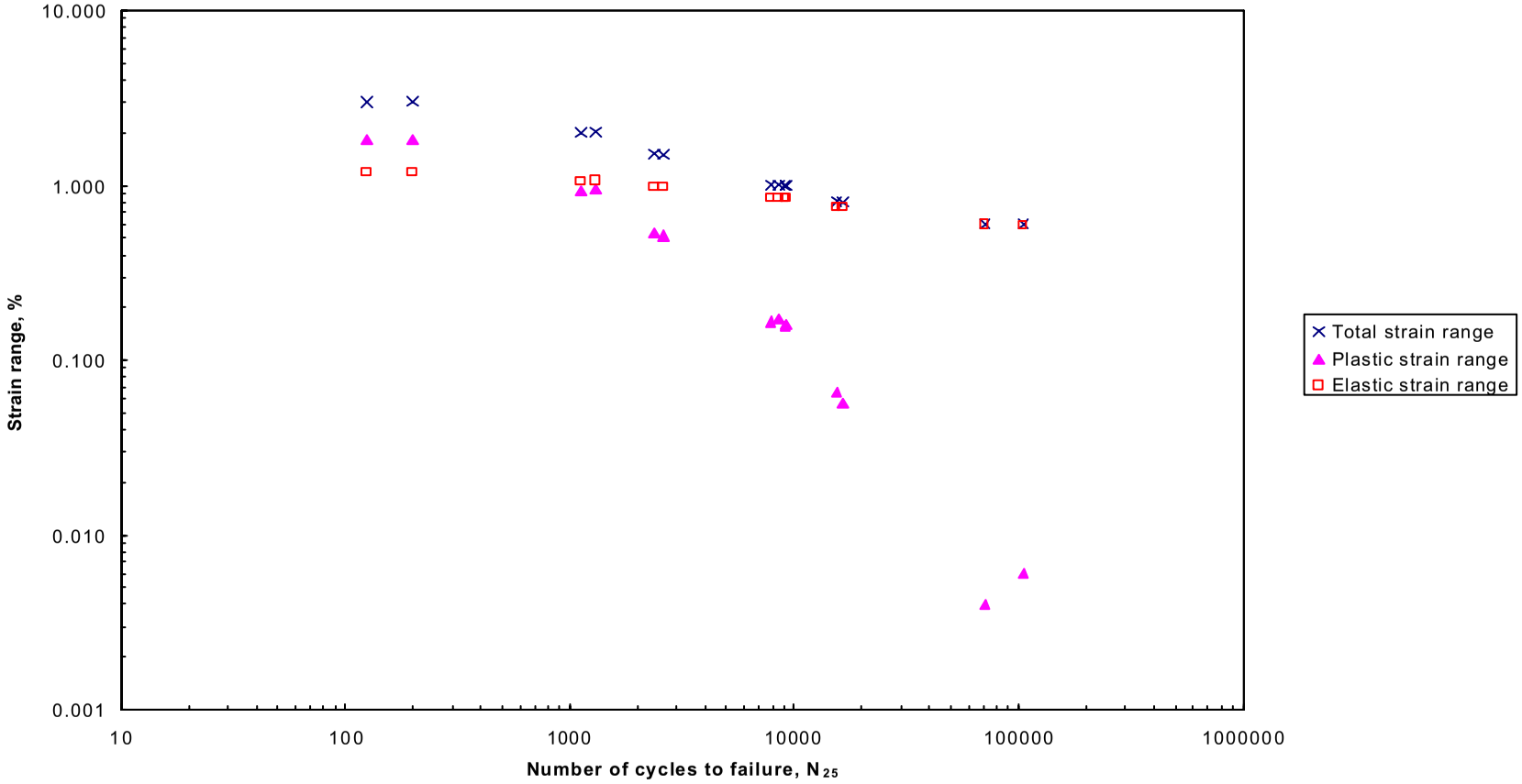

Figure 19. Baseline fatigue curves in terms of the total, plastic and elastic strain ranges for tests at ambient temperature

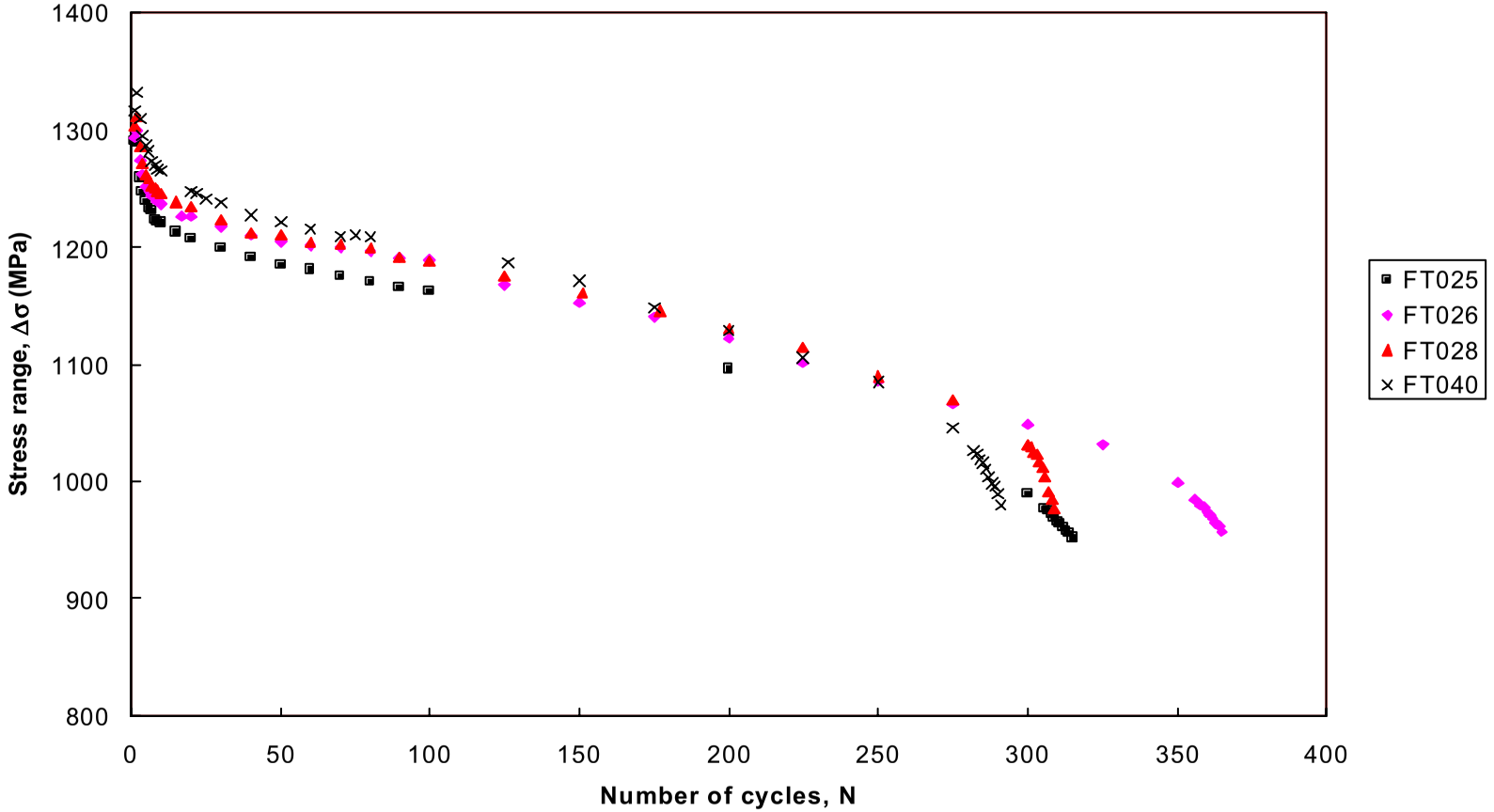

Figure 20. Examples of the deformation behaviour curves for Nimonic 101 at 850°C (baseline data; repeat tests at $\Delta\varepsilon_t$ = 1.2%)

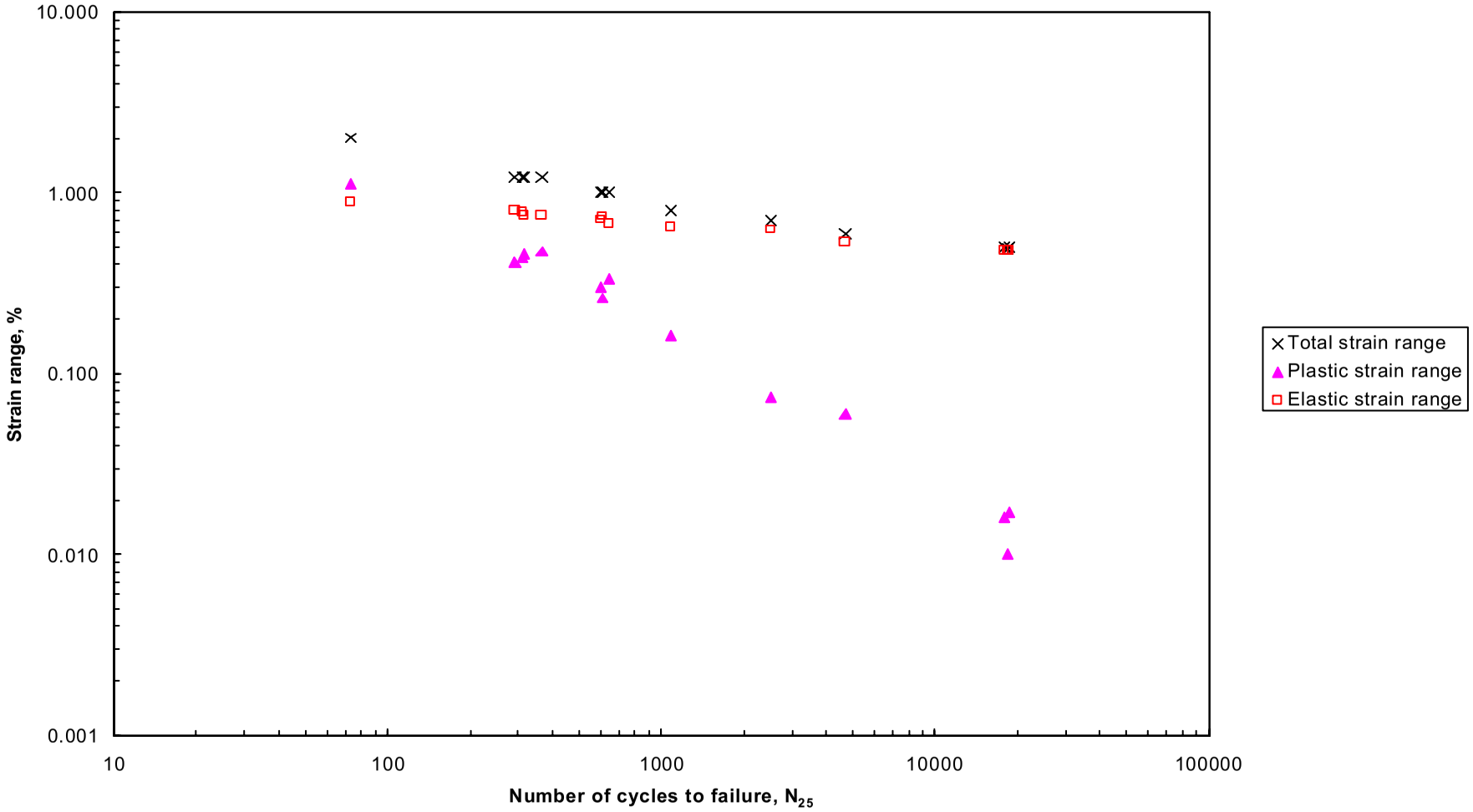

Figure 21. Baseline fatigue life curves at 850°C

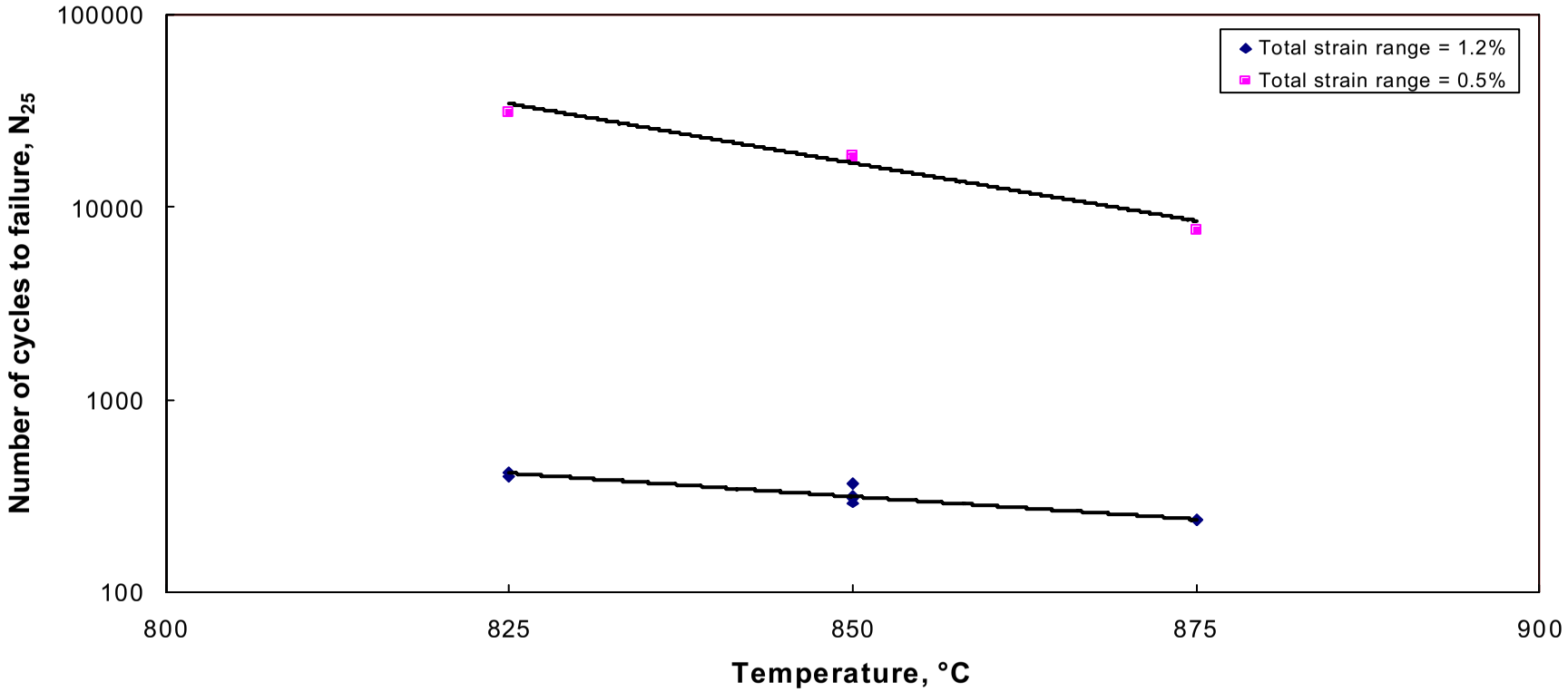

Figure 22. Variation of the fatigue life with the test temperature

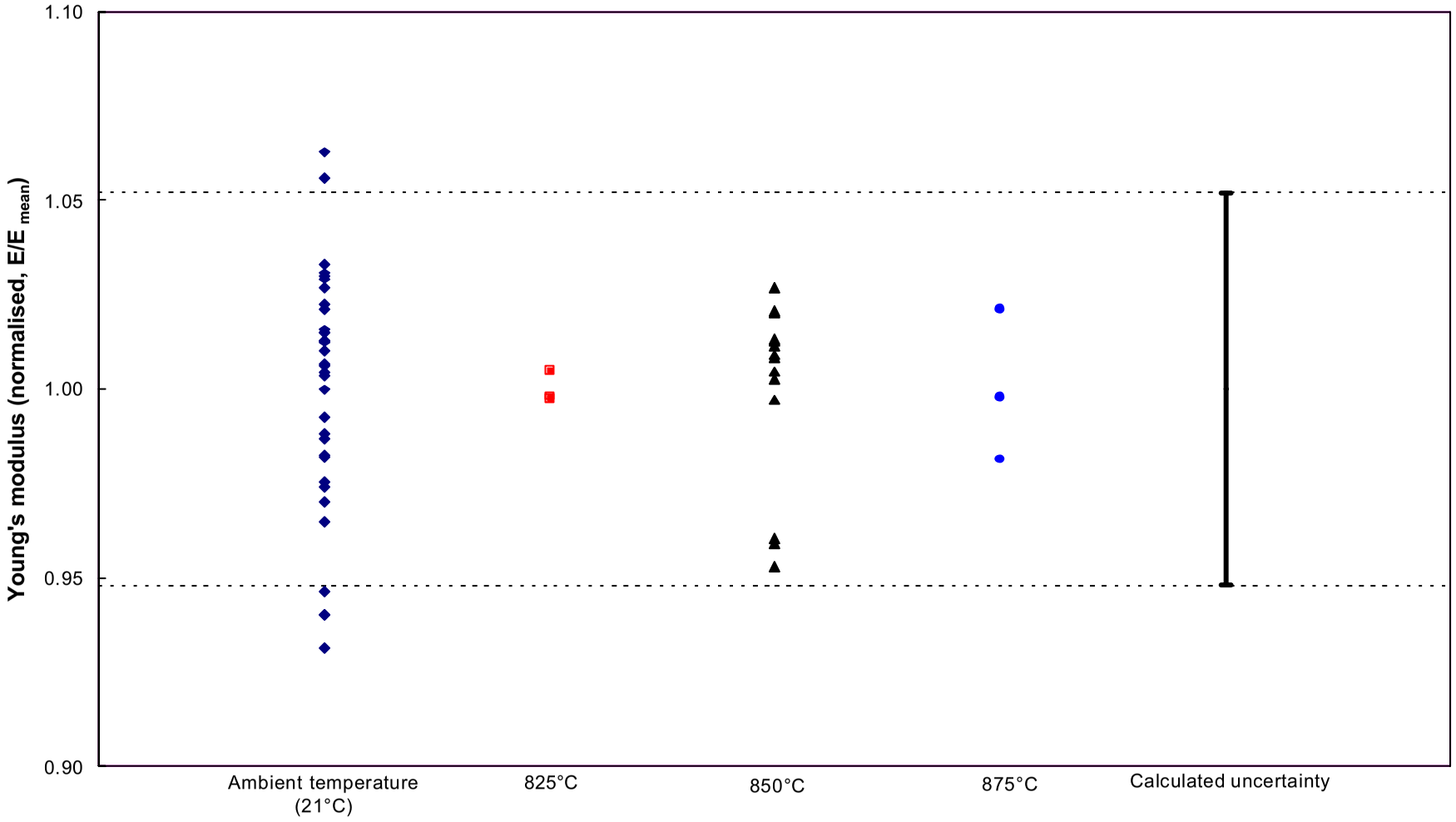

Figure 23. Comparison of the spread in measured Young's modulus results with the estimated uncertainty (Shown are the estimated 95% uncertainty limits in Table 10)

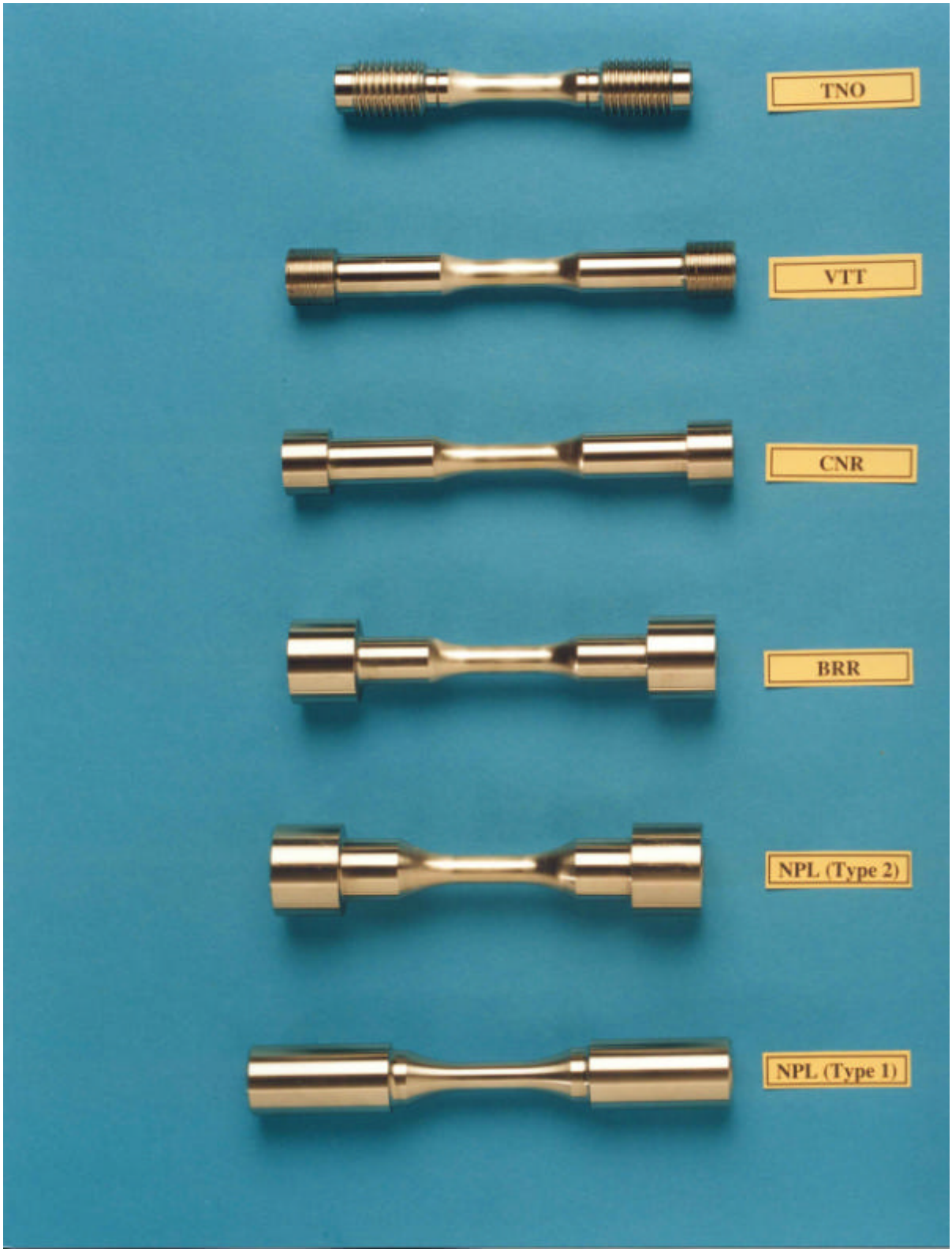

Figure 24. Specimen geometries used in inter-laboratory tests at ambient temperature

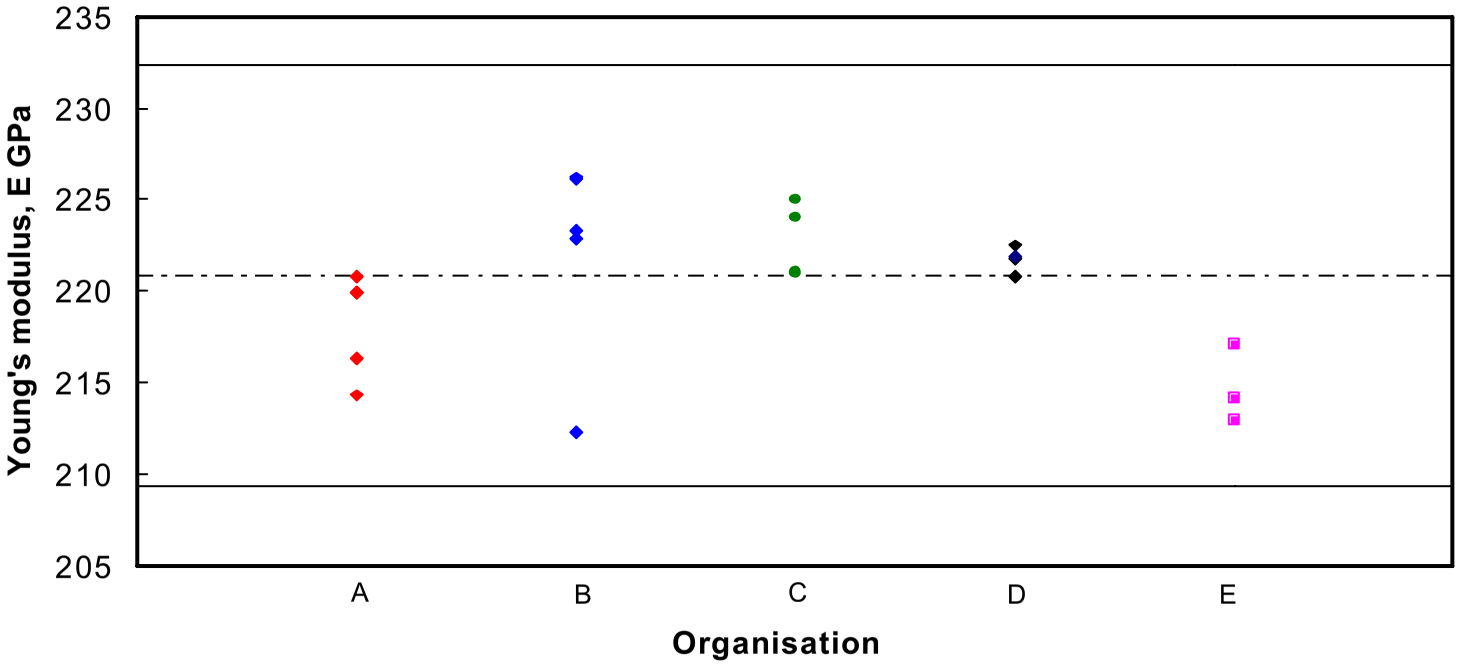

Figure 25. Inter-laboratory results of Young's modulus measurements at ambient temperature (Also shown are the estimated 95% uncertainty limits based on the baseline data - Table 10)

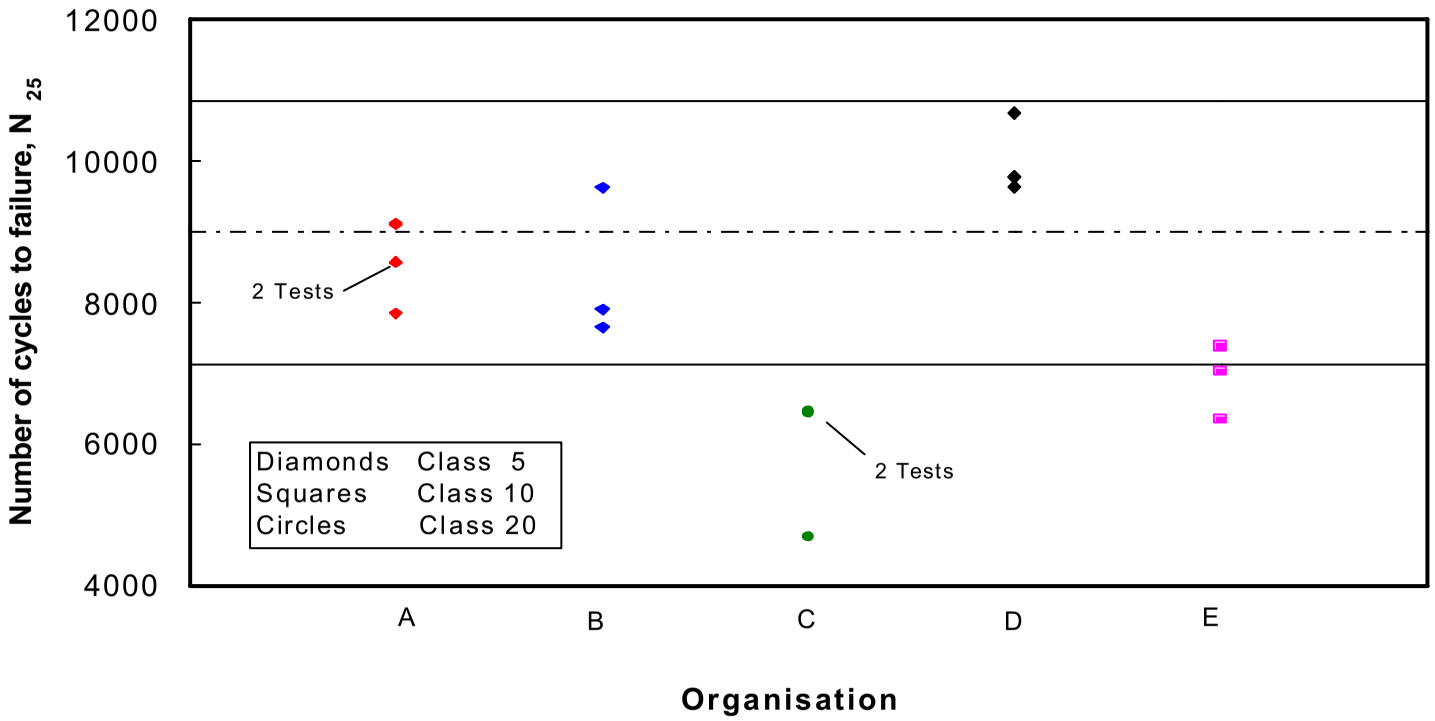

Figure 26. Inter-laboratory comparison of lifetime results for strain-controlled tests at ambient temperature and $\Delta\varepsilon_t$ = 1.0% [Also shown are the estimated 95% uncertainty limits based on the data for Partners A, B & D – Table 11]

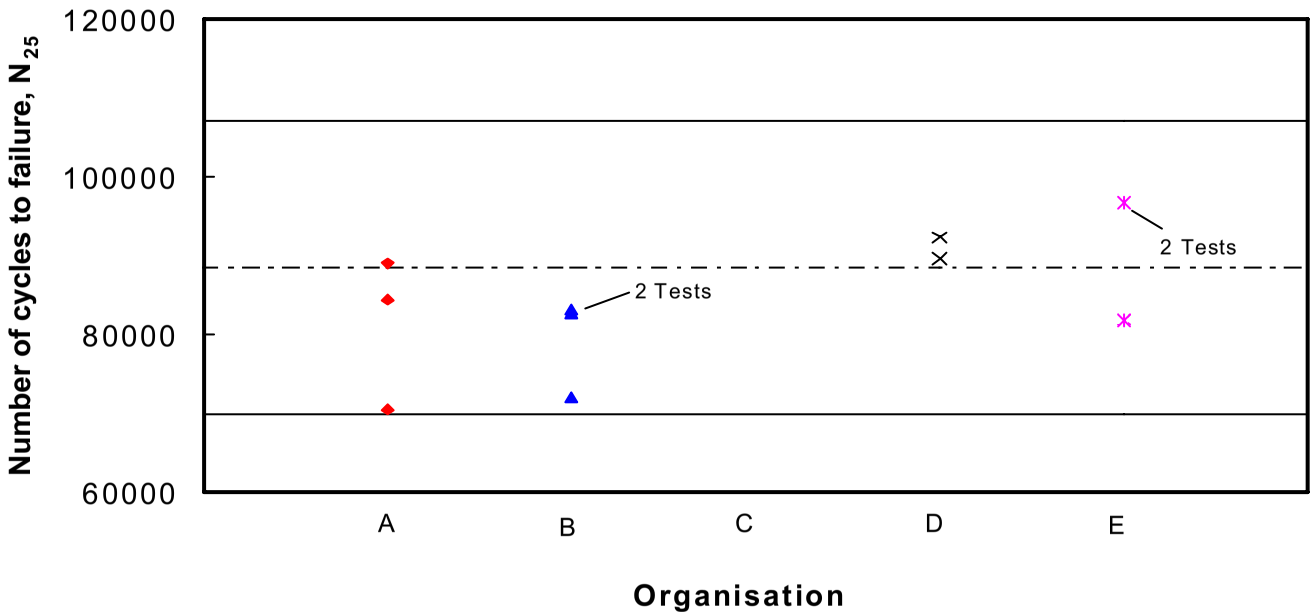

Figure 27. Inter-laboratory comparison of fatigue life for stress-controlled tests at ambient temperature and $\Delta\sigma$= 1200 MPa [Also shown are the estimated 95% uncertainty limits based on the data for Partners A, B & D – Table 12]

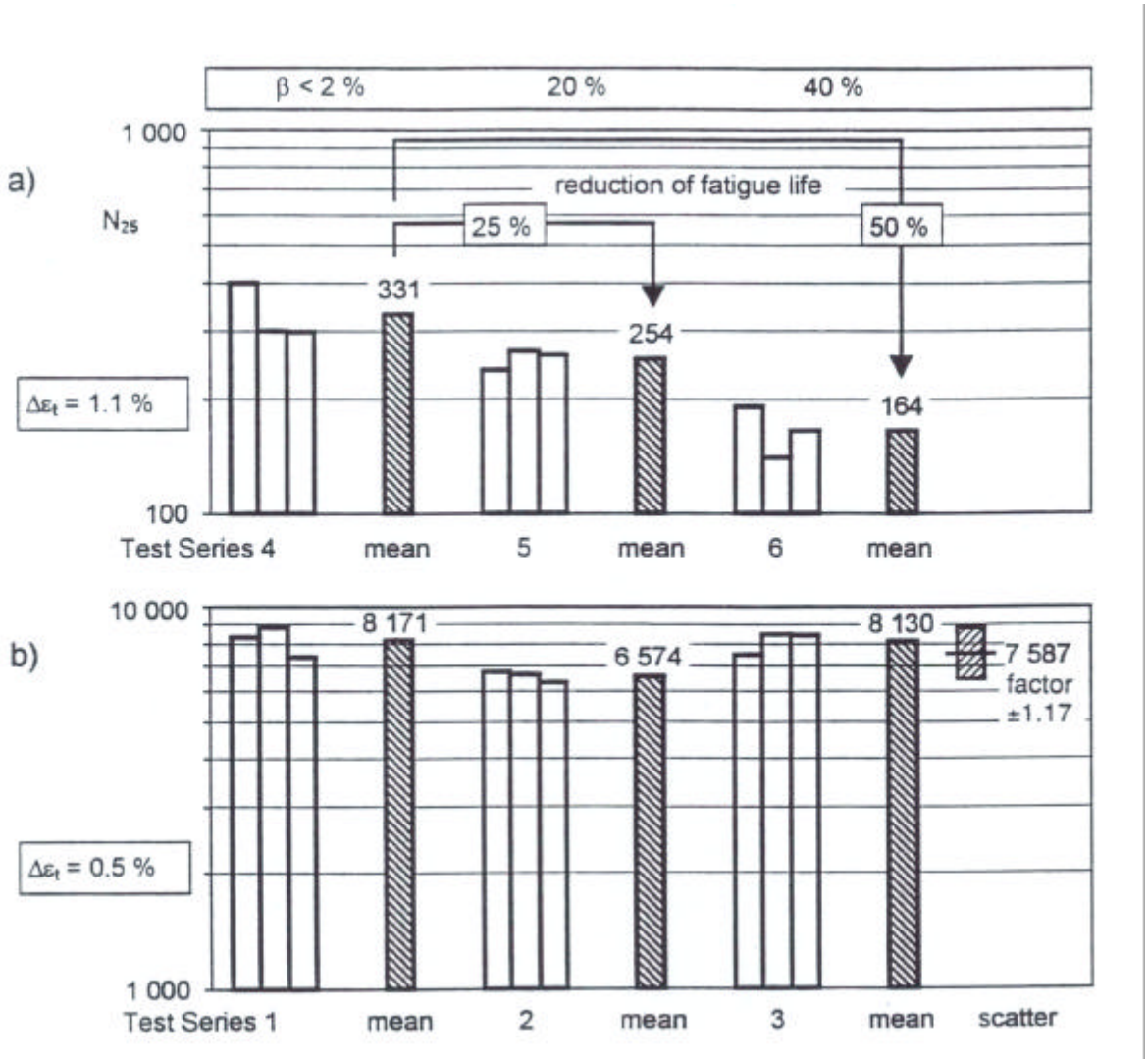

Figure 28. Comparison of fatigue life under different levels of specimen percent bending; see Scholz [14]

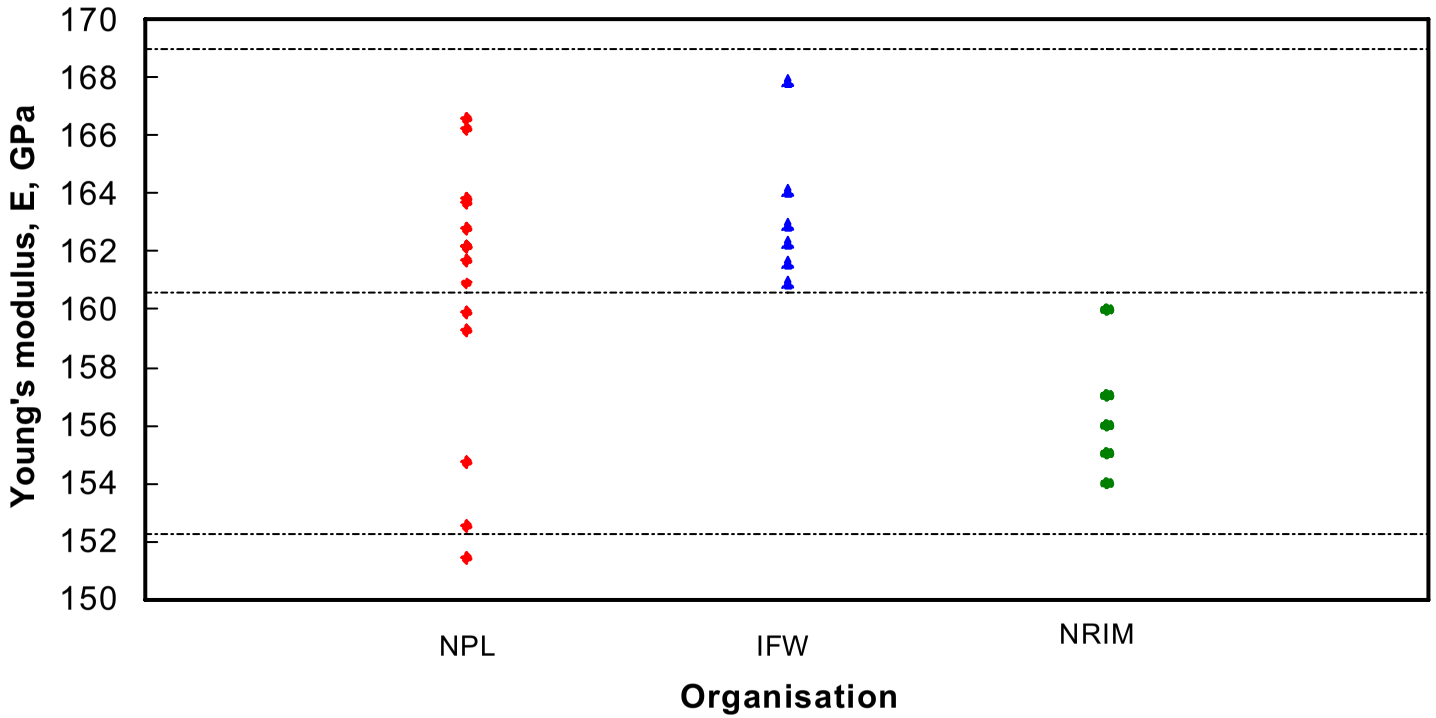

Figure 29. Inter-comparison of Young's modulus at 850°C
[Also shown are the estimated 95% uncertainty limits based on the baseline data - Table 10]

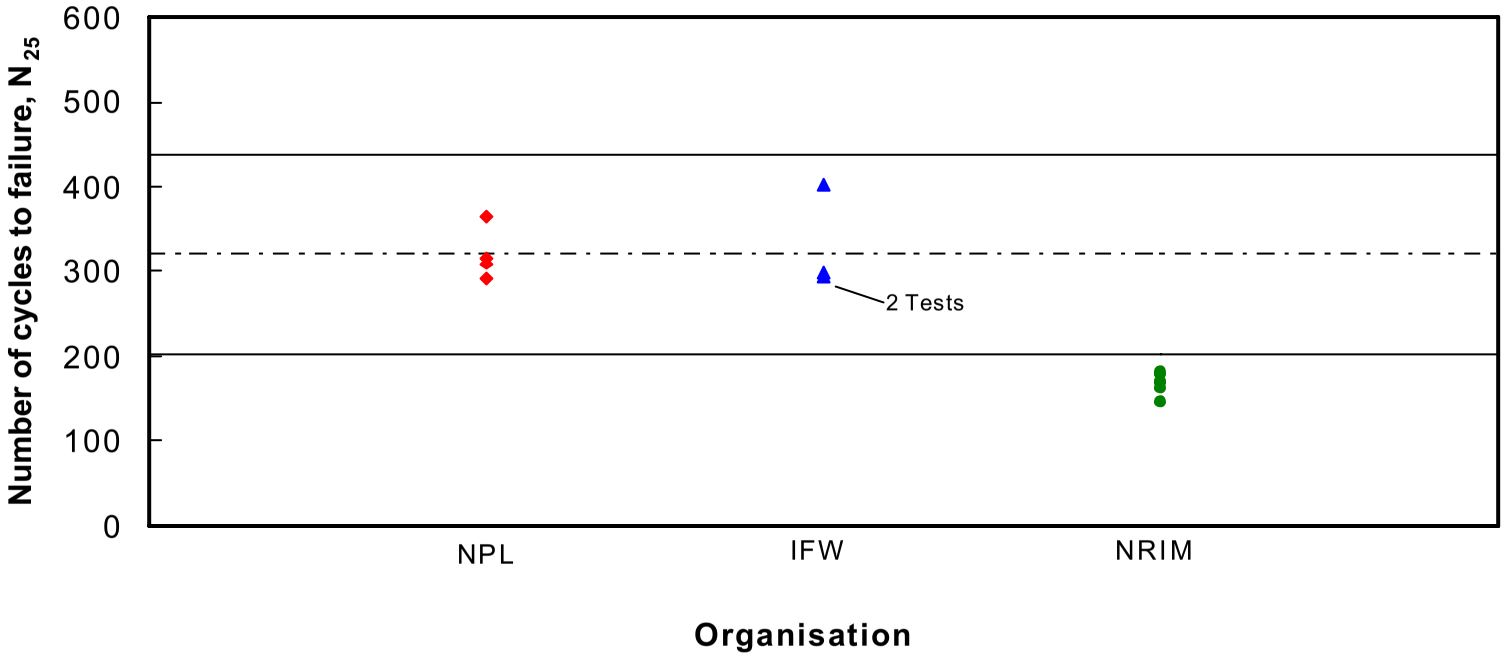

Figure 30. Inter-comparison of fatigue life at 850°C, $\Delta\varepsilon_t$ = 1.2% (IFW $\Delta\varepsilon_t$ = 1.1%)
(Also shown are the estimated 95% uncertainty limits based on the baseline data – Table 13)

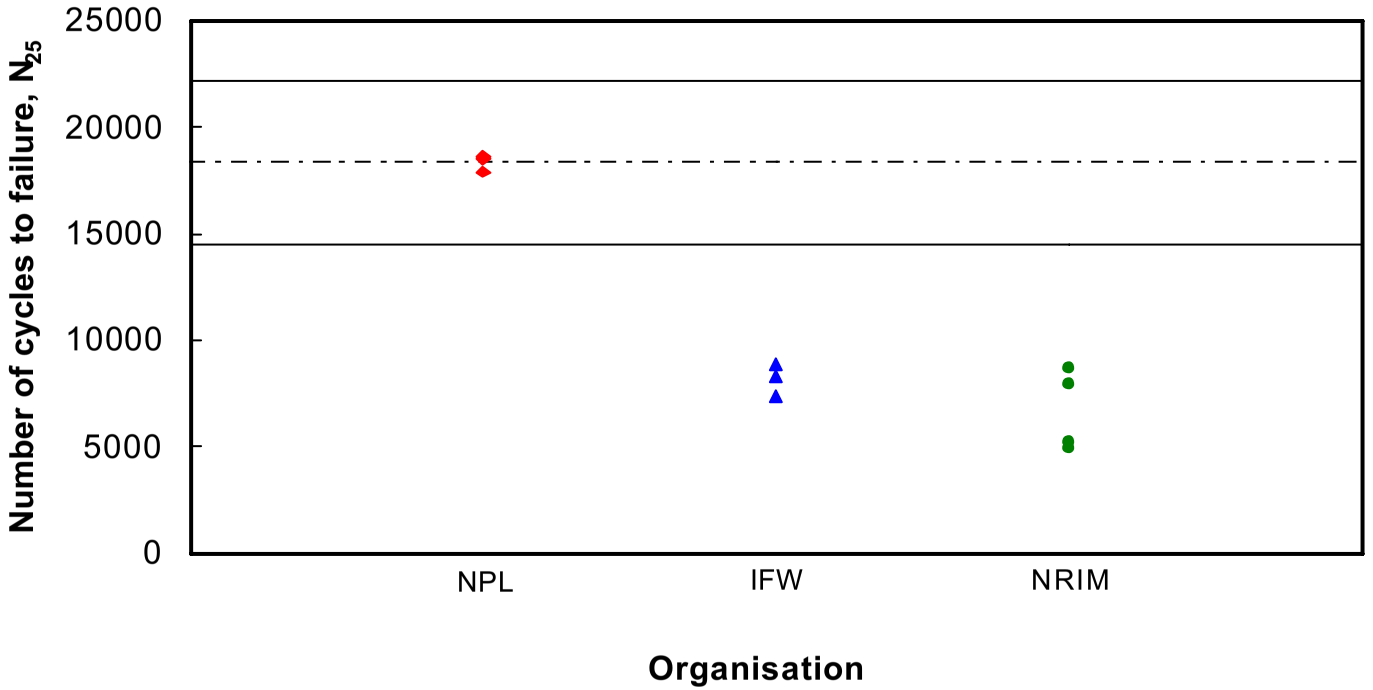

Figure 31. Inter-comparison of fatigue life at 850°C, $\Delta\varepsilon_t$ = 0.5%.
(Also shown are the estimated 95% uncertainty limits based on the baseline data - Table 14)

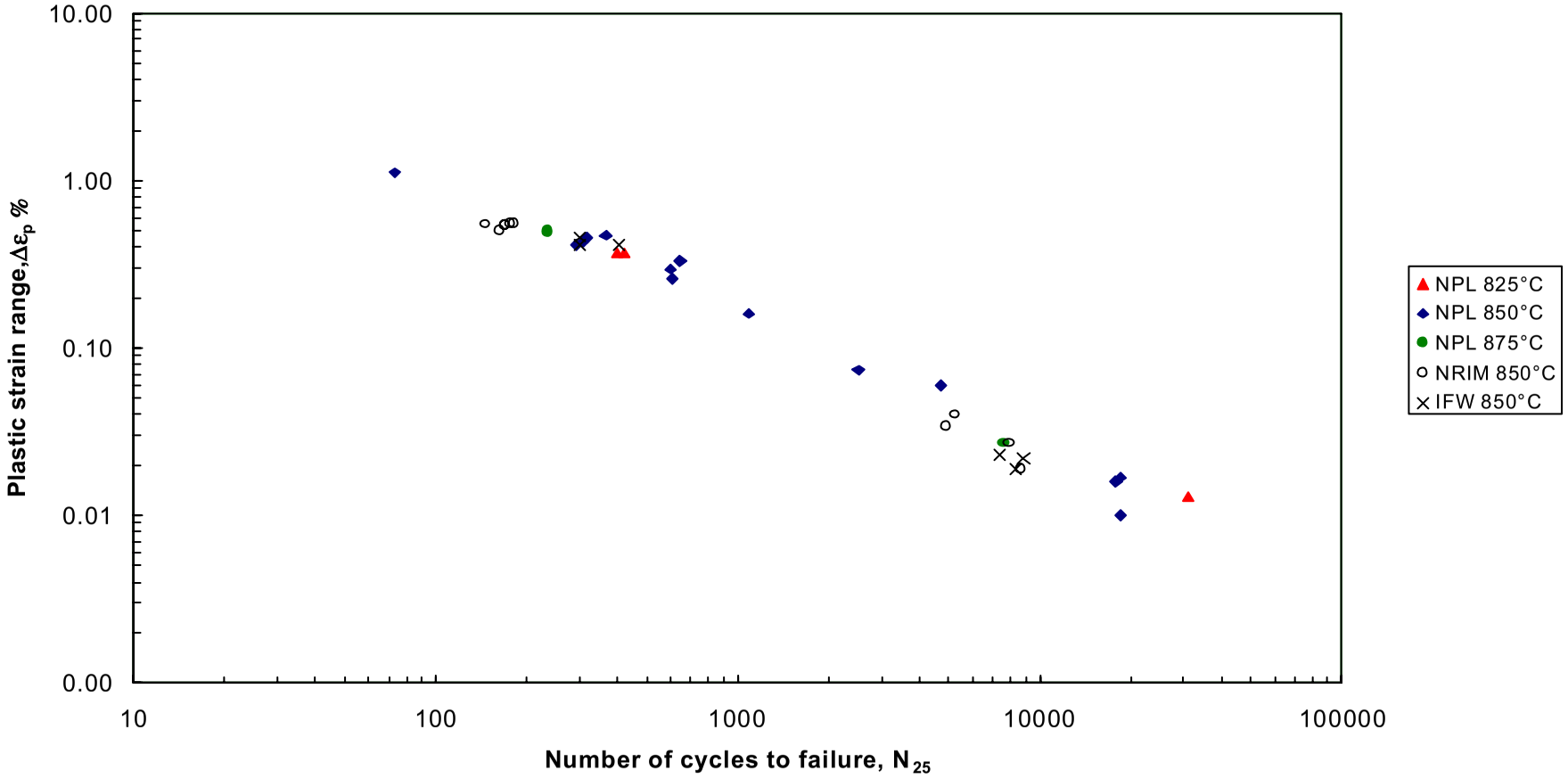

Figure 32. Fatigue life as a function of the plastic strain range (all results within the temperature range 825°C to 875°C)

APPENDIX A: MACHINING INSTRUCTIONS FOR LCF SPECIMENS

1. Cut specimen blank to length.

2. Centre-drill each end to the same depth.

3. Rough machine the outside diameter to the grip end size plus 0.25 mm on the diameter.

4. Machine the intermediate section down to its nominal size plus 0.25 mm in diameter using a depth-of-cut per pass of 0.5 mm.

5. Machine the centre profile to its true size plus 0.25 mm on diameter using a depth-of-cut per pass of 0.2 mm.

6. By grinding, finish the grip ends, then the intermediate-shoulder parts.

7. Finish the centre profile section to the true size.
NOTE: From 0.1 mm of the final diameter, the rate of material removal must not exceed 0.005 mm per pass (transverse-grinding) and no more than 0.001 mm per turn (plunge-grinding).

8. Engrave the identification mark on both ends of the specimen.

9. Finish the specimens by mechanical polishing in the longitudinal direction to produce a surface roughness, R_a, not exceeding 0.10 µm. This can be achieved by using a Morrison Specimen Polishing machine with 800 grit papers for 15 minutes followed by 1000 grit paper for approximately 20 minutes.

General Notes:

NOTE 1. Perform all machining operations between centres.

NOTE 2. Use suitable lubricant with sufficient flow to prevent heating of the surface and continually remove the abrasive particles from the lubricant. The grinding wheel must be frequently dressed as necessary.

NOTE 3. As the specimen cannot be given a permanent identification mark until after the final machining is complete, some form of temporary identification (i.e. kept in individually marked bags or boxes) must be maintained.